DISSERTATIONES
CHIMICAE
UNIVERSITATIS
TARTUENSIS
196

LARISA IVANOVA

Design of active compounds against neurodegenerative diseases

DISSERTATIONES CHIMICAE UNIVERSITATIS TARTUENSIS
196

DISSERTATIONES CHIMICAE UNIVERSITATIS TARTUENSIS
196

LARISA IVANOVA

Design of active compounds against neurodegenerative diseases

UNIVERSITY OF TARTU
Press

Institute of Chemistry, Faculty of Science and Technology, University of Tartu, Estonia

The dissertation was accepted for the commencement of the degree of Doctor of Philosophy in Molecular Engineering on June 12th, 2020, by the Doctoral Committee of the Institute of Chemistry, University of Tartu.

Supervisors: Prof. Mati Karelson,
Institute of Chemistry, University of Tartu, Estonia

Jaana Tammiku-Taul, PhD,
Institute of Chemistry, University of Tartu, Estonia

Opponent: Prof. Dan Lindholm, PhD MD
Institute of Biomedicine, University of Helsinki, Finland

Commencement: August 26th, 2020 at 10:15, Ravila 14a, Tartu, room 1020

This work has been partially supported by Graduate School of Functional materials and technologies receiving funding from the European Regional Development Fund in University of Tartu, Estonia.

ISSN 1406-0299
ISBN 978-9949-03-392-8 (print)
ISBN 978-9949-03-393-5 (pdf)

University of Tartu Press
www.tyk.ee

TABLE OF CONTENTS

LIST OF ORIGINAL PUBLICATIONS 7

ABBREVIATIONS 8

INTRODUCTION 9

1. LITERATURE OVERVIEW 11
   - 1.1. Current protein targets used for *in silico* drug design against neurodegenerative diseases 11
   - 1.2. Neurotrophic factors in the therapy of neurodegenerative diseases 12
   - 1.3. Glial cell line-derived neurotrophic factor 13
   - 1.4. Earlier attempts to find small-molecule mimetics of neurotrophic factors 13
   - 1.5. Earlier attempts to find multiple target drug candidates against neurodegenerative diseases 14

2. AIMS OF THE STUDY 16

3. MODELLING AND EXPERIMENTS 17
   - 3.1. Computational methods 17
     - 3.1.1. Computational methods in drug design 17
     - 3.1.2. Preparation of protein target structures and small-molecule ligands 17
     - 3.1.3. Molecular docking and virtual screening 19
     - 3.1.4. Molecular dynamics simulations 20
     - 3.1.5. Binding energy estimation by MM/GBSA method 21
   - 3.2. Enzyme inhibition assays 22

4. RESULTS AND DISCUSSION 23
   - 4.1. GDNF mimetics 23
     - 4.1.1. Molecular modelling of the interactions between GDNF family receptor GFRα1 and small-molecule ligands 24
     - 4.1.2. Novel small-molecule ligands as potential GDNF family receptor agonists 29
   - 4.2. Combination of QSAR and molecular modelling methods 34
     - 4.2.1. Identification of natural compounds against neuro-degenerative diseases using *in silico* techniques 35
     - 4.2.2. Potential multitarget candidates against Alzheimer's disease 39

SUMMARY 43

REFERENCES 45

SUMMARY IN ESTONIAN 58

ACKNOWLEDGEMENTS 60

PUBLICATIONS 61
CURRICULUM VITAE 139
ELULOOKIRJELDUS 141

LIST OF ORIGINAL PUBLICATIONS

The thesis is based on the four original papers, listed below:

I. **Ivanova, L.**; Tammiku-Taul, J.; García-Sosa, A.T.; Sidorova, Y.; Saarma, M.; Karelson, M. Molecular dynamics simulations of the interactions between glial cell line-derived neurotrophic factor family receptor GFRα1 and small-molecule ligands. *ACS Omega* **2018**, *3(9)*, 11407–11414.

II. **Ivanova, L.**; Tammiku-Taul, J.; Sidorova, Y.; Saarma, M.; Karelson, M. Small-molecule ligands as potential GDNF family receptor agonists. *ACS Omega* **2018**, *3(1)*, 1022–1030.

III. **Ivanova, L.**; Karelson, M.; Dobchev, D.A. Identification of natural compounds against neurodegenerative diseases using in silico techniques. *Molecules* **2018**, *23(8)*, 1847.

IV. **Ivanova, L.**; Karelson, M.; Dobchev, D.A. Multitarget approach to drug candidates against Alzheimer's disease related to AChE, SERT, BACE1 and GSK3β protein targets. *Molecules* **2020**, *25(8)*, 1846.

Author's contribution:

I. The author carried out molecular docking and molecular dynamics simulations, participated in analysis of modelling results, and contributed to writing the manuscript.

II. The author carried out molecular docking and molecular dynamics simulations, participated in analysis of modelling results, and contributed to writing the manuscript.

III. The author was responsible for molecular modelling, analysing results, and writing the respective part of the manuscript.

IV. The author was responsible for molecular modelling, planning and performing experimental measurements, analysing results, and writing the respective part of the manuscript.

ABBREVIATIONS

Aβ	Amyloid-β
AD	Alzheimer's disease
AChE	Acetylcholinesterase
ALS	Amyotrophic lateral sclerosis
ANN	Artificial neural network
BACE1	Beta-site amyloid precursor protein cleaving enzyme 1
BMLR	Best multilinear regression
CADD	Computer-aided drug design
Ex/Em	Excitation/emission
GDNF	Glial cell line-derived neurotrophic factor
GFL	GDNF family ligands
GFRα1	GDNF family receptor alpha 1
GSK3β	Glycogen synthase kinase 3β
HD	Huntington's disease
HTVS	High-throughput virtual screening
IC_{50}	Half maximal inhibitory concentration
LE	Ligand efficiency
LRRK2	Leucine-rich repeat kinase 2
MD	Molecular dynamics
MM/GBSA	Molecular mechanics generalised Born surface area
NMDA	*N*-methyl-D-aspartate receptor
OPLS	Optimised potentials for liquid simulations
PD	Parkinson's disease
PDB	Protein data bank
pY	Phosphorylation
QSAR	Quantitative structure–activity relationship
RESPA	Reversible reference system propagator algorithm
RMSD	Root-mean-square deviation
SBDD	Structure-based drug design
SERT	Serotonin transporter
SPC	Simple point charge
TrkA	Tropomyosin receptor kinase A
WHO	World Health Organization

INTRODUCTION

Neurodegenerative diseases represent a wide range of diseases of various nature, caused by the gradual death of certain groups of nerve cells and characterised by steadily progressing neurological deficits, including motor disorders, psychoemotional, and cognitive (up to dementia) disorders. The most common neurodegenerative diseases are Alzheimer's disease (AD), Parkinson's disease (PD), Huntington's disease (HD), and amyotrophic lateral sclerosis (AML). Currently, the world has seen a rapid increase in patients with neurodegenerative diseases. According to a report by the World Health Organization (WHO) [1,2], the total number of people with dementia worldwide amounted to 47 million in 2015, increasing to 75 million by 2030, and up to 132 million by 2050. According to the WHO, AD and other forms of dementia are also among the ten leading causes of death in the world [3].

The main feature of these diseases is their long-term asymptomatic development, and the clinical symptoms characteristic of each disease appear after the almost complete degradation of the key regulatory neurons and the depletion of compensatory brain reserves. To date, the exact cause of neuronal death during neurodegeneration is unknown, however, some genetic and environmental factors have been associated with this type of disease. The main factors include the life expectancy and environmental pollution [4]. There are presently no radical treatments for the neurodegenerative disorders. Current methods of the treatment are symptomatic and aim to increase the activity of surviving neurons in order to minimise the clinical manifestations of the degenerative process.

Neurological diseases have a significant impact not only at the individual level but also on the whole society, since the treatment and rehabilitation of patients places a heavy financial burden on society and the state. Thus, in 2015 the worldwide dementia costs amounted to $818 billion, and by 2030, the cost of caring for people with dementia is estimated to have risen to $2 trillion [2].

The rapid growth of patients, the increase in the cost of treatment and support for those suffering from neurodegenerative diseases and their loved ones, the increase in life expectancy, and the consequent ageing of the population make the fight against neurodegenerative diseases one of the major global challenges of the 21st century [5]. In the fight against neurodegeneration, several approaches are currently being used to create and search for drugs with neuroprotective properties.

1) Directed construction of drugs using rational computer design based on the knowledge about the molecular mechanisms of the pathogenesis of neurodegenerative diseases [6,7].
2) Search among available medicines, regardless of their field of application [8].
3) Isolation of physiologically active substances with neuroprotective properties from body tissues and their chemical modification [9].

4) A combination of the above three approaches, structural and conformational optimisation of a drug molecule [10].

This thesis provides examples of the use of modern methods of molecular modelling in the development of new drugs against neurodegenerative diseases as well as the use of computational chemistry methods to study and understand the mechanisms of action of potential drug candidates with their biological targets.

1. LITERATURE OVERVIEW

1.1. Current protein targets used for *in silico* drug design against neurodegenerative diseases

With an improvement in the quality of life and medical services, life expectancy is also increasing, which in turn leads to an ageing population and the spread of age-related diseases, particularly neurodegenerative diseases. Many organisations and individual laboratories are working on the development of treatment for neurodegenerative diseases, but there is still no effective therapy and drugs. The main obstacles are the complexity of the brain and its working mechanisms, the insufficient availability of resources and ethical limitations. Nevertheless, in recent decades, advances in computer technology have allowed *in silico* experiments to have a significant impact on the development of novel drugs and drug candidates [11–13].

Nowadays, computer-aided drug design (CADD) is widely exploited in the development of new drugs. The first step in this approach is the identification of the target protein. A sufficient number of protein targets have been found to be directly or indirectly associated with neurodegenerative diseases [14]. Such a variety of potential targets arises from the fact that most neurodegenerative diseases are characterised by multiple disorders. The target proteins that have been currently used in computer design are listed in Table 1.

Table 1. Current protein targets related to neurodegenerative diseases and used for *in silico* approaches.

Disease	Targets	Computationally derived drugs	Ref.
AD	AChE	Flavonoid derivatives, macluraxanthone, kaempferol, rutin, quercetin, pyridopyrimidine, 6-chloro-pyridonepezil, pyridonepezil, and piperazine derivatives	[15,16]
	BuChE	-	[11,17]
	NMDA	Memantine	[18]
	BACE1	AF267B, OM00-3 and OM99-2	[19,20]
	SERT	-	[21]
	GSK3β	-	[22]
	Muscarinic and nicotinic AChE receptors	-	[23]
	γ-Secretase: presenilin I	-	[24,25]
	Calcium-permeable AMPA receptors (CP-AMPARs)	-	[26,27]

Table 1. (continued)

Disease	Targets	Computationally derived drugs	Ref.
PD	LRRK2	LRRK2 kinase inhibitors, pyrroloquinoline quinone, dopamine related compounds	[28]
	SNCA	-	[29]
	PINK1	-	[30]
	PARK2	-	[17]
	DJ-1	-	[31]
ALS	Copper-zinc superoxide dismutase	Hesperidin, 2,3,5,4'-tetrahydroxystilbene-2-O-β-D-glucoside (THSG)	[32,33]
	CASP-3	-	[34]
	CDC7	-	[35]
	p38 MAPK	-	[36]
	SCN8A	Riluzole	[37]
HD	HTT-interacting protein 1	-	[38]
	Postsynaptic density-95	-	[39]
	FIP-2	-	[40]

1.2. Neurotrophic factors in the therapy of neurodegenerative diseases

Neurotrophic factors are essential proteins that regulate the proliferation, survival, and differentiation of cells in the peripheral and central nervous system [41]. At the same time the neurotrophic factors have neuroprotective functions. Neurotrophic factors comprise three families of growth factors: the NGF family (neurotrophins) [42], glial cell line–derived neurotrophic factor (GDNF) family ligands [43], and the heterogeneous group of molecules that belong to the cytokine family [44]. More recently, unconventional neurotrophic factors, such as cerebral dopamine neurotrophic factor (CDNF) and mesencephalic astrocyte-derived neurotrophic factor (MANF), have been described [45].

The high potency of neurotrophic factors as well as their role in survival of neurons makes them rational therapeutic agents for neurodegenerative diseases. However, their clinical use is limited because of difficulties in protein delivery and pharmacokinetics in the central nervous system [46]. The first clinical trials involving neurotrophic factors as drugs were conducted back in the 1990s, but none of them received permission from the authorities due to the lack of specific targeting, difficulties in achieving an effective dose, and side effects [47]. Unsuccessful clinical trials led to a reassessment of the suitability of neurotrophic factors in neurodegenerative diseases as well as to a more thorough study of the physiological basis of the pharmacology of neurotrophic factors as a potential biological target on the development of neuroprotective drugs [48].

1.3. Glial cell line-derived neurotrophic factor

Glial cell line-derived neurotrophic factor (GDNF) is the first identified member of the GDNF family of ligands (GFL) and was primarily isolated from the rat B49 glial cell line in 1993. Structurally, GDNF is a glycosylated and disulphide-bonded homodimer with the molecular weight approximately 33–45 kDa [49]. The GDNF signalling is mediated by a multicomponent receptor complex consisting of RET receptor tyrosine kinase and a glycosyl phosphatidylinositol (GPI)-linked ligand-binding subunit known as GDNF family receptor α (GFRα) [50]. GDNF specifically binds to GFRα1. The complex of homodimers of GFL and GFRα1 brings two molecules of RET together, triggering transphosphorylation of specific tyrosine residues in their tyrosine kinase domains and intracellular signalling [51]. RET, in turn, activates several intracellular signalling cascades, which regulate cell survival, differentiation, proliferation, migration, chemotaxis, branching morphogenesis, neurite outgrowth, and synaptic plasticity.

GDNF promotes the survival of several types of neurons, such as dopaminergic and motor neurons [52]. The GDNF signalling has also an important role in the kidney development [53] and spermatogenesis [54]. GDNF has a neuroprotective effect and induces fiber outgrowth as demonstrated in rat and primate models of PD [55-59]. It was also shown in rat model of ALS that *ex vivo* gene delivery of GDNF slows degeneration of the motoneurons [60]. Forlenza *et al.* demonstrated that the GDNF level decreases in Alzheimer's patients, especially those with cognitive impairments [61]. The injection of GDNF into the brain of rabbits protected them against Alzheimer's-like symptoms caused by aluminium exposure [62]. GDNF has also beneficial effect in the case of age-related neuron damage [63,64]. In the clinical trials of GDNF, beneficial effects have been described for patients, which have been followed for longer periods, but the method of delivery of the protein into brain has become a critical issue [65-67].

1.4. Earlier attempts to find small-molecule mimetics of neurotrophic factors

As described in Section 1.2, the use of neurotrophic factors and their receptors in the treatment of neurodegenerative diseases has several problems and constraints. Subsequently, many studies of neurotrophic factors as therapeutic targets in neurodegenerative diseases were concentrated on the search for small molecules that have a selective effect and mimic the effect of neurotrophic factors. Thus, Saragovi *et al.* suggested that selective Trk-activating agents that circumvent p75 binding and activation would be neuroprotective. They created small-molecule mimetics of neurotrophins [68-75], agonistic monoclonal antibodies (mAbs) [76-79], and small-molecule mimetics of the mAbs [75-82] that exhibited neuroprotective activity *in vivo*. Later, other groups have reported about several TrkB small-molecule agonists, and TrkB and TrkC agonistic mAbs that demonstrate the protective effect in the 1-methyl-4-phenyl-1,2,3,6-

tetrahydropyridine (MPTP) neurotoxicity mouse model of PD [83-89] and in the transgenic R6/2 and BACHD mouse models of HD [90,91]. One of the Trk-selective small-molecule agonists found by Saragovi *et al.* is presently in Phase 3 clinical trials for an ophthalmic indication, TrkC-selective mAb agonist is in preclinical studies for ALS, and Trk-selective agonistic mAbs and neurotrophins mutants are under investigation for neurosensory hearing loss [48].

The small-molecule agents related to other neurotrophic factors have been also reported. In 2003, Tokugawa *et al*. described compound XIB4035 as a GFRα1 agonist [92], but it was later shown to be a GFRα1 modulator, able to potentiate signalling in the presence of GDNF [93,94]. Doonan *et al.* found that the synthetic progestin Norgestrel has a neuroprotective effect in the rat model of retinal degeneration diseases (Retinitis Pigmentosa) [95]. Sidorova *et al*. demonstrated that small-molecule agonists of GFRα1, BT13, and BT18 have RET modulatory activity and efficiency in rat model of neuropathy [93,96].

Although the first clinical trials with neurotrophic factors were initiated 25 years ago, the applicability of neurotrophic factors in the treatment of neurodegenerative diseases is currently unclear [97]. Thus, the development of small-molecule mimetics or agonists of neurotrophic factors is of great interest, the use of small-molecule compounds may facilitate the achievement of the required pharmacokinetic properties and biological activity.

1.5. Earlier attempts to find multiple target drug candidates against neurodegenerative diseases

Alzheimer's disease (AD) is the most common neurodegenerative disorder for which there are currently no effective drugs. The development of new therapies is hindered because a deeper understanding of the exact pathophysiology and molecular mechanism of AD is lacking. The pathological features of AD include amyloid deposition [98], astrogliosis [99], tau protein hyperphosphorylation and accumulation [100,101], neuronal dystrophy [102], oxidative stress [103], biometal dyshomeostasis, decline in acetylcholine levels [104], *etc*. Because a variety of potential biological targets has been related to this disease, the identification of multitarget compounds against AD is one of the promising approaches in the drug development [105]. The multitarget drugs acting simultaneously against several adverse factors of AD could be more effective and may possess a safer profile compared to single-target drugs.

Several attempts have been made to find multitarget compounds against AD. Sharma *et al.* had carried out virtual screening using molecular docking and molecular dynamics and identified several *N*-benzylpiperidine analogues that have inhibitory activity against AChE and BACE1 [106]. A series of hydroxylated chalcones were computationally designed and synthesised by Cong *et al.* as dual-functional compounds that inhibit simultaneously the amyloid-β (Aβ) peptide aggregation as well as the ferroptosis [107]. Fang *et al.* developed some tetrahydroisoquinoline-benzimidazoles that inhibited BACE1 and ex-

hibited significant anti-neuroinflammatory activity and good blood-brain barrier penetration in artificial membrane permeation assay [108]. Proceeding from computational molecular docking and molecular dynamics simulations, Gonzalez-Naranjo *et al.* had developed a new family of indazolylketones with a multitarget profile against cholinesterase and BACE1. Altogether nine indazolylketones with significant multifunctional activity against the above targets were discovered. The subsequent pharmacological tests showed that some of indazolylketones of the final set act as CB2 cannabinoid agonists and simultaneously inhibit of BuChE and/or BACE1 [109]. Novel isoflavone analogues were found in the work by Wang *et al.* as multitarget-directed ligands for histamine 3 receptor (H3R) and AChE [110]. Despite limited initial success, the multitarget approach remains a very promising direction in the development of novel drugs.

2. AIMS OF THE STUDY

The main objective of this thesis is the application of the different molecular modelling techniques in drug discovery against neurodegenerative diseases. This work is focused on the development and search for new drug candidates against the most common neurodegenerative diseases, namely Alzheimer's and Parkinson's diseases.

Paper I The main objective of this paper is the study of the possible mechanism of interaction between the known agonists and the GFRα1-RET complex using molecular modelling techniques;

Paper II The aim of this paper is the molecular design of the potential GFRα1 agonists using the structure-based drug design;

Paper III The aim of this paper is to identify new potentially active compounds for three protein targets (TrkA, NMDA, and LRRK2) using a combination of different QSAR and molecular modelling methods;

Paper IV The aim of this paper is a development and application of a combination of the QSAR and molecular modelling methods in the design of multitarget drug candidates against Alzheimer's disease.

3. MODELLING AND EXPERIMENTS

3.1. Computational methods

3.1.1. Computational methods in drug design

The process of finding and developing drugs is a rather time-consuming and expensive process. Over the past three decades, computer-based drug detection and design methods have played an increasingly significant role in the development of new therapeutically active compounds. The computer-aided drug design (CADD) methods help to accelerate the long process of developing new medicines and reduce their cost. Notably, CADD technology has played an important role in the discovery of many pharmaceutical products that have been approved by the regulatory agencies and reached the consumer market [111,112]. The principal tools for rational drug design include molecular docking and the related virtual screening of large chemical compound libraries, molecular dynamics (MD) simulations and quantitative structure–activity relationship (QSAR) methods, such as multilinear regression or machine learning. The molecular docking and molecular dynamics belong to the class so-called target-based methods, whereas QSAR makes the foundation of ligand-based methods. The research in the present thesis was carried out using mostly the target-based methods. The technical details of the application of these methods are described in the following sections of this Chapter.

3.1.2. Preparation of protein target structures and small-molecule ligands

The initial step in using the molecular modelling methods is the preparation of protein target structures and small-molecule ligands. The raw crystal structures of protein targets are available from Protein Data Bank (PDB) [113]. A list of the crystal structures of proteins used in the present thesis is given in Table 2.

Before modelling, all reported crystal structures of proteins were pre-treated using Schrödinger Protein Preparation Wizard [114]. Hydrogen atoms were automatically added to the proteins and water molecules were removed. In Paper **I**, the 2D chemical structures of the small-molecule ligands were converted into the 3D structures and optimised by molecular mechanics MM+ field using HyperChem 8.0 [115]. PDB files for molecular docking were created using the "Online SMILES Translator and Structure File Generator" [116]. In Papers **III** and **IV**, the 3D structures of the ligands were generated using LigPrep procedure from the Schrödinger Suite [117]. The OPLS_2005 force field of LigPrep was used in all ligand preparation steps. Generation of all possible states and ionisation states was enumerated for each ligand using Epik at a pH of 7.0 ± 2. PDB files were created from lowest energy conformers for

each ligand. PDBQT files for molecular docking procedure were generated from the corresponding PDB files using the AutoDock Tools software [118].

Table 2. List of the used crystal structures of the studied proteins.

PDB ID	Name	Resolution, Å	Method	Released	Ref.
4UX8	GDNF-GFRα1-RET complex	24	Electron microscopy	2014	[119]
3FUB	GDNF-GFRα1 complex	2.35	X-ray diffraction	2009	[120]
4U8Z	MST3 in complex with a pyrrolopyrimidine inhibitor (PF-06447475)	1.63	X-ray diffraction	2015	[121]
5TP9	Human GluN1/GluN2A LBD in complex with GNE9178	2.4	X-ray diffraction	2016	[122]
4AOJ	Human TrkA in complex with the inhibitor AZ-23	2.75	X-ray diffraction	2012	[123]
4EY6	Human AChE in complex with (-)-galantamine	2.39	X-ray diffraction	2012	[124]
6EQM	Human BACE-1 in complex with CNP520	1.35	X-ray diffraction	2018	[125]
1PYX	Human GSK-3 beta in complex with AMP-PNP	2.4	X-ray diffraction	2003	[126]
5I6X	ts3 human SERT in complex with paroxetine	3.14	X-ray diffraction	2016	[127]

3.1.3. Molecular docking and virtual screening

Molecular docking is a widely used computational method in drug design. The essence of this method is to model the relative position between a small molecule (ligand) and a studied target protein (receptor). Currently, a variety of software packages is available for molecular docking [128]. To find the best binding mode between a small molecule and a receptor, a molecular docking algorithm takes into account the geometric complementarity and flexibility of a ligand and/or a receptor as well as their interatomic interactions (i.e., hydrogen bonds and hydrophobic contacts). Each docking procedure is based on a specific search algorithm, such as incremental construction (IC) [129,130], genetic algorithm (GA) [131,132], Monte Carlo [133], *etc*. After obtaining the best orientation using a scoring function (Dock Score, Glide Score, Chem Score, *etc*. [134,135]), which approximately describes the interaction energy of a small molecule with a target protein, the docking program ranks the studied substances.

In Papers **I** and **II**, the molecular docking was carried out using AutoDock Vina 1.1.2 (hereinafter referred to as Vina) [136] that applies an iterated local search global optimiser [137,138]. A series of steps consisting of the geometry optimisation is executed in order to obtain the ligand-receptor complex conformation with the lowest binding energy. Each step is validated according to the Metropolis criterion [136]. For the local geometry optimisation, the Vina software uses Broyden-Fletcher-Goldfarb-Shanno (BFGS) [139] method. The BFGS, like other quasi-Newton optimisation methods, uses not only the value of the interaction energy but also its gradient, i.e., the derivatives of the scoring function with respect to its arguments. The final binding ligand-protein conformation is characterised by its energy E_{bind}, free energy ΔG_{bind} or ligand efficiency LE:

$$LE(E) = \frac{E_{bind}}{N_h} \tag{1}$$

$$LE(\Delta G) = \frac{\Delta G_{bind}}{N_h} \tag{2}$$

where N_{h} denotes the number of non-hydrogen atoms in the ligand.

In Paper **IV**, Vina was used for the high throughput virtual screening (HTVS) [140] of the chemical compound libraries. During the screening, the docking parameters were used in their default values. After the HTVS procedure, the results were automatically sorted from lowest to highest energy, and compounds with binding energy highest than -8.0 kcal/mol were excluded from further analysis [141].

In Papers **III** and **IV**, the HTVS was carried out using the Glide virtual screening workflow module of the Schrödinger Suite (hereinafter referred to as Glide HTVS) [142,143] that applies a series of hierarchical filters to search for possible locations of the ligand in the active-site region of the receptor. At the

next step, Glide produces a set of initial ligand conformations that are selected from an exhaustive enumeration of the minima in the ligand torsion-angle space and are represented in a compact combinatorial form. Based on these ligand conformations, initial screens are executed throughout the phase space available to the ligand to determine the location of the perspective positions of the ligand. This pre-screening significantly reduces the region of phase space over which computationally expensive energy and gradient evaluations will be later done, while avoiding the use of stochastic methods [144]. Glide is a force-field based docking program that uses an optimised potential for liquid simulations, e.g. OPLS force fields. The potential energy of the system is represented as a sum of bond, angle, torsion, and nonbonded terms in the OPLS family of force fields [145-149]. Molecular geometry and vibrational frequencies are mainly determined by the bond and angle terms and the torsion term describes the energetics of conformational rearrangement of the system. The nonbonded terms include electrostatic interactions calculated using atom-centred partial charges and a Lennard-Jones potential [150] representing dispersion and electronic repulsion.

The Glide HTVS procedure includes three steps: (i) docking with HTVS precision level, (ii) docking with standard precision level, and (iii) docking with an extra precision. All small-molecule ligands were docked flexibly with five docking poses generated for each ligand. Only the best scoring pose was kept for the next step. After each step, the top 30% of ligands with the best docking score were automatically selected for the next step. In this way, a set of 500 compounds for each target were obtained.

In Papers **III** and **IV**, the binding interfaces of studied proteins were identified using Schrödinger Glide Grid Generation [151]. The obtained data were also used for docking/virtual screening with Vina.

3.1.4. Molecular dynamics simulations

The molecular dynamics (MD) simulations are one of the most powerful computational methods to model physical and biological systems. Molecular dynamics methods allow to calculate the classical trajectories of individual atoms and to study the dynamics of the interaction of particles in condensed systems at the molecular level. The molecular dynamics has been widely used to study the structural and dynamic properties of proteins, nucleic acids, lipid membranes, *etc*. In Papers **I**–**IV**, the MD simulations were used to study in detail the binding of small molecules to the target proteins.

The simulations were carried out using Desmond program package of Schrödinger LLC [152]. The simulations were executed in cubic simple point charge SPC [153] water box using OPLS_2005 force field parameters (see Section 3.1.3) [154]. Sodium and chloride ions were placed in the solvent to a concentration 0.15 M, thereafter, to achieve electroneutrality, additional ions were added to the system. The isothermal-isobaric (NPT) ensemble with the temperature 300 K and a pressure 1 bar was applied in all runs. The simulation

length was 50 ns with relaxation time 1 ps for each studied protein–protein complex conformation. The long-range electrostatic interactions were calculated using the particle mesh Ewald (PME) method [155]. The cutoff radius in Coulomb interactions was 9.0 Å. The Martyna-Tuckerman-Klein chain coupling scheme [156] with a coupling constant of 2.0 ps was used for the pressure control and the Nosé-Hoover chain coupling scheme [156] for the temperature control. Nonbonded forces were calculated using a reversible reference system propagator algorithm (RESPA) integrator, where the short-range forces were updated every step and the long-range forces were updated every three steps. The trajectories were saved at 50 ps intervals. The behaviour and interactions between the proteins were analysed using the Simulation Interaction Diagram tool implemented in Desmond molecular dynamics package. The stability of MD simulations was monitored by checking the root-mean-square deviation (RMSD) of the protein atom positions in time.

3.1.5. Binding energy estimation by MM/GBSA method

The binding free energy is an important property characterising various (bio)molecular processes, such as protein folding, molecular association, interactions between small-molecule ligands and proteins, *etc*. Therefore, an accurate assessment of the free energy is one of the most important tasks in biomolecular studies. The theoretical calculations of the free energies of biomolecular systems by numerical simulation are becoming more and more widespread, as the experimental measurements of the thermodynamic properties of these systems can be often cumbersome and time-consuming [157]. In CADD, the binding free energy is used to characterise the binding strength between a receptor and a small-molecule ligand. Different theoretical methods of binding free energy calculations, especially the end-point methods have been successfully used in drug design [161-163]. These methods are based on samplings of the final states of a system, being much less expensive than using molecular dynamics and more accurate than most docking scoring functions. The molecular mechanics Poisson-Boltzmann surface area (MM/PBSA) and molecular mechanics generalised Born surface area (MM/GBSA) methods developed by Kollman *et al.* are the most frequently used end-point free energy methods [164-166]. These methods have been used to evaluate docking poses, determine structural stability, and predict binding affinities of the ligand-receptor complexes.

MM/PBSA and MM/GBSA utilise the decomposition of the free energy of binding [167-169] into the individual terms arising from the following sum:

$$G = E_{bind} + E_{el} + E_{vdW} + G_{pol} + G_{np} - TS \quad (3)$$

where the first three terms are standard MM energy terms from bonded (bond, angle, dihedral), electrostatic, and van der Waals interactions, respectively. G_{pol}

and G_{np} are the polar and nonpolar contributions to the solvation free energies, respectively. In MM/GBSA approach, G_{pol} is obtained using the generalised Born (GB) model [170], whereas the nonpolar term is estimated from a linear relation to the solvent accessible surface area of the ligand. The last term in the equation (3) is the absolute temperature (T), multiplied by the entropy (S), estimated from the normal-mode analysis of the vibrational frequencies.

3.2. Enzyme inhibition assays

In Paper **IV**, the activity of the selected compounds against AChE, BACE1, and GSK3β was evaluated using commercially available assay kits, i.e., AChE inhibitor screening colorimetric kit (BioVision), human β-secretase (BACE1) inhibitor fluorometric screening kit (BioVision), and GSK3β assay kit (BPS Bioscience) with Kinase-Glo (Promega) as a detection reagent. The concentration range of all tested compounds was selected based on the QSAR predictions (see Table S3 in Supplementary Material for Paper **IV**). All experiments were executed according to the manufacture's protocols in three parallels in 96-well plates. For the spectroscopic measurements, Synergy M microplate reader (BioTek, USA) or GloMax 96 microplate luminometer (Promega, USA) were used.

In the AChE inhibitor screening kit, an active *h*AChE enzyme hydrolyses the colorimetric substrate, generating a yellow chromophore, which can then be detected by absorbance at 412 nm in kinetic mode at room temperature for 40 min.

In the *h*BACE1 inhibitor screening kit, the activity of compounds is measured by their ability to inhibit the cleavage of a BACE1-specific substrate. The cleavage of the substrate by *h*BACE1 results in a product with high fluorescence that is registered in kinetic mode at 37 ºC for 90 min at Ex/Em = 345/500 nm.

In the GSK3β assay kit, the kinase activity is measured by quantification of the amount of ATP remaining in solution following the kinase reaction. The generated luminescent signal is correlated with the amount of ATP in solution and inversely to the kinase activity.

The values of the IC_{50} were calculated using GraphPad prism version 8.0 for Windows [171].

4. RESULTS AND DISCUSSION

4.1. GDNF mimetics

As described in Section 1.2, the GDNF family ligands (GFLs) are of interest as potential therapeutic agents against neurodegenerative diseases. However, the use of these ligands has several problems due to their relatively large size, limited delivery to the central nervous system through the blood-brain barrier, low pharmacokinetic properties and bioavailability, and potential side and off-target effects [37].

Thus, the development of small molecules that mimic the effect of GFLs and activate the RET signalling pathway can solve most of these problems. As mentioned in Section 1.3, three small-molecule ligands that mimic neurotrophic effects of GDNF and may act as GFRα1 agonists have been currently reported: XIB4035 [92], BT13 [93], and its derivative BT18 [96] (Figure 1). Despite the proven activity of these compounds, their molecular mechanism of the RET activation is still unclear. In Paper **I**, potential binding sites of BT13 and BT18 agonists in the GFRα1–RET complex were studied in detail using molecular docking and molecular dynamics simulations. In Paper **II**, a potential GFRα1 agonist showing a different binding mode to the GFRα1–RET complex as compared to BT13 and BT18 was designed using the structure-based drug design (SBDD) approach.

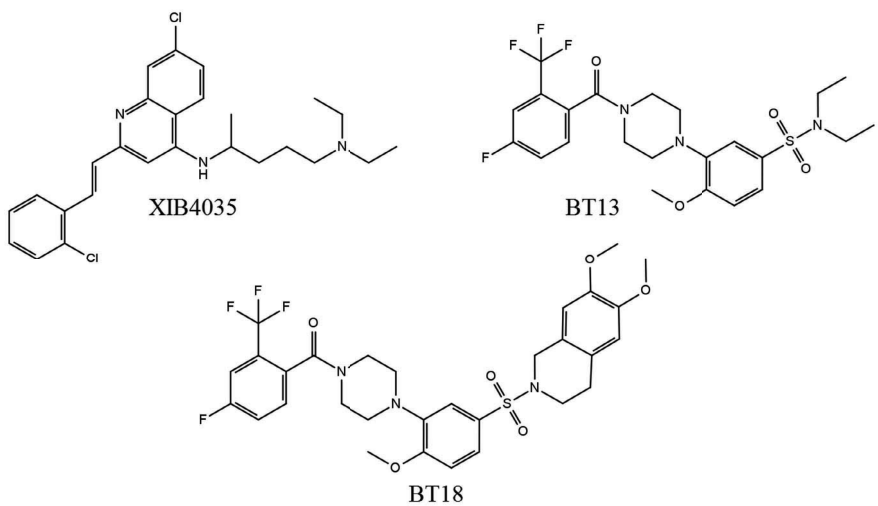

Figure 1. Chemical structures of small-molecule ligands XIB4035, BT13, and BT18.

4.1.1. Molecular modelling of the interactions between GDNF family receptor GFRα1 and small-molecule ligands

In Paper **I**, a possible mechanism of action of the known GFRα1 agonists was elucidated based on the computational molecular modelling. The crystal structure of GDNF–GFRα1–RET complex (PDB ID: 4UX8 [119]) was used in this study. Three possible binding regions were examined in this complex: a potential binding site of GFRα1 with GDNF as region A; a potential binding site of RET (cadherin-like domains 1 and 2) with GFRα1 as region B; and a potential allosteric binding site in the middle of GFRα1 as region C (Figure 2). The crystal structure of GDNF–GFRα1 complex with a higher resolution (PDB ID: 3FUB [120]) was used as a control.

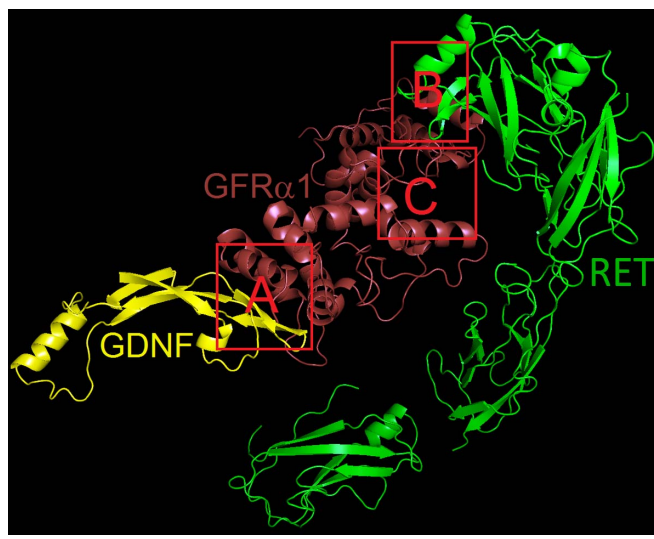

Figure 2. Potential binding sites in the GDNF–GFRα1–RET complex (PDB ID: 4UX8).

According to the molecular docking calculations, the lowest binding energy positions for both small-molecule ligands BT13 and BT18 were found at the allosteric site in binding region of GFRα1. The docking scores were: -7.9 kcal/mol for compound BT13, being 1.9 and 1.2 kcal/mol lower than for regions A and B, respectively; -9.8 kcal/mol for compound BT18, being 3.4 and 2.3 kcal/mol lower than for regions A and B, respectively. The compound BT13 formed a hydrogen bond by its sulphonyl group with the ammonium group of Lys327 of GFRα1, together with several hydrophobic contacts in region C (Figure 3E). The compound BT18 had a hydrogen bond between its methoxy group and the amine group of Asn40 as well as several hydrophobic interactions in region C (Figure 3F).

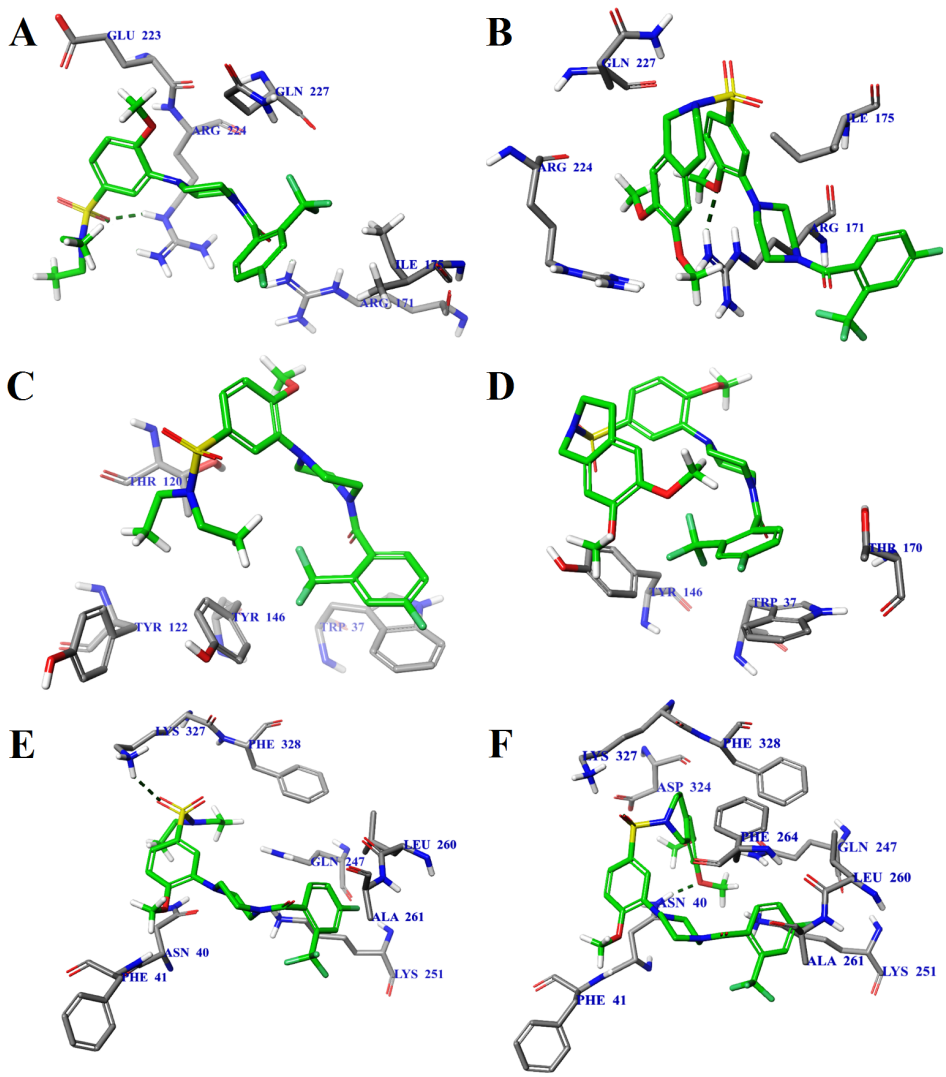

Figure 3. Calculated binding modes of the protein-ligand complexes: (A) GFRα1-BT13 at the GDNF–GFRα1 interface, region A; (B) GFRα1–BT18 at the GDNF–GFRα1 interface, region A; (C) RET–BT13 at the RET–GFRα1 interface, region B; (D) RET-BT18 at the RET–GFRα1 interface, region B; (E) GFRα1–BT13 at the allosteric site, region C; and (F) GFRα1–BT18 at the allosteric site, region C. Intermolecular hydrogen bonds are shown by green dashed lines.

It should be noted that experimentally compounds BT13 and BT18 also act as RET direct agonists [93,96], although our calculations showed that the allosteric site of GFRα1 is the preferable binding region for both ligands. The binding site at RET interface with GFRα1 (region B) may become preferential in

membrane-bound state of RET, with altered conformation as compared to the protein structure in the single-particle state registered in the X-ray measurements (PDB ID: 4UX8 [119]). Both ligands showed stacking (π-π) interactions with Trp37 and had hydrophobic contacts with some residues of RET in region B (Figure 3C,D).

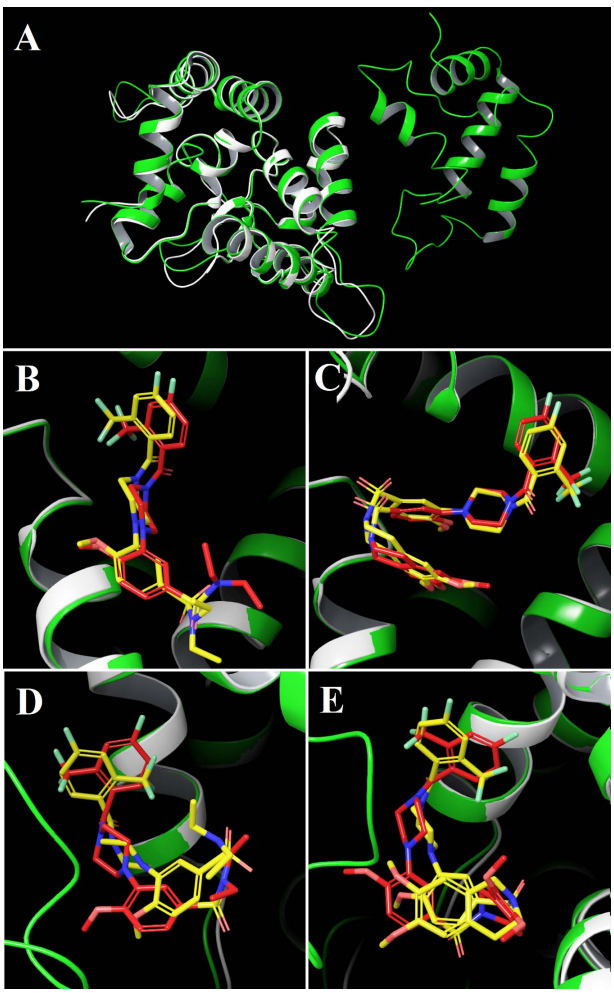

Figure 4. Comparison of the binding of compounds BT13 and BT18 to protein structures 4UX8 (green) and 3FUB (white). (A) Structural alignment of protein structures; (B) compound BT13 at the GDNF–GFRα1 interface, region A; (C) compound BT18 at the GDNF–GFRα1 interface, region A; (D) compound BT13 at the allosteric site of GFRα1, region C; (E) compound BT18 at the allosteric site of GFRα1, region C. In each graph (B–E), the ligand conformation with protein structure 3FUB is in yellow and the ligand conformation with protein structure 4UX8 in red.

The comparison of binding poses for compounds BT13 and BT18 was carried out using the crystal structure of GDNF–GFRα1 complex (PDB ID: 3FUB [120]) and the results are presented in Figure 4. The binding modes of both ligands were almost identical at the GDNF−GFRα1 interface (Figure 4B,C), but somewhat different at the allosteric site (Figure 4D,E). This difference can be explained by the fact that the full structure of GFRα1 consists of three domains (D1, D2, and D3) in 4UX8 [119], however, GFRα1 in 3FUB does not have domain D1 that is not needed for GDNF binding [46], but it binds to RET. The full analysis of all binding modes is given in Table S1 in the Supporting Information of Paper **I**.

The docking calculations were followed by the MD simulations of compounds BT13 and BT18 at the three potential binding sites in regions A, B, and C of the GFRα1, respectively. The RMSD variations of the atomic positions were used for estimating the stability of the ligand binding. The MD calculated variations of this parameter were significantly larger for the complexes of compounds BT13 and BT18 in regions A and B as compared to the binding in region C of GFRα1. The RMSD of the complexes in region C were 6.4 Å for BT13 and 8.0 Å for BT18, respectively (see Figure S1a-f in the Supporting Information of Paper **I**). Thus, in accordance with the molecular docking results, the MD simulations also predicted the allosteric binding site in region C as preferable for compounds BT13 and BT18.

The amino acid residual structure of the binding modes of ligands BT13 and BT18 was also identified using the MD simulations. An analysis of the interactions between the ligands and the protein at the allosteric site showed that the compound BT13 formed hydrogen bonds with the amino acid residues Phe41 and Thr265 of GFRα1, complemented with significant hydrophobic contacts around protein residues Lys251 to Phe264, and several interactions over the water molecule bridges (Figure 5A). The computational model of the compound BT18 binding mode showed its long-term hydrophobic contact with the protein residue Phe41 (almost 100% of the simulation time), some other hydrophobic interactions around protein residues Leu244 to Phe264, several water-assisted interactions, and a specific π-cation contact with Lys251 (Figure 5B).

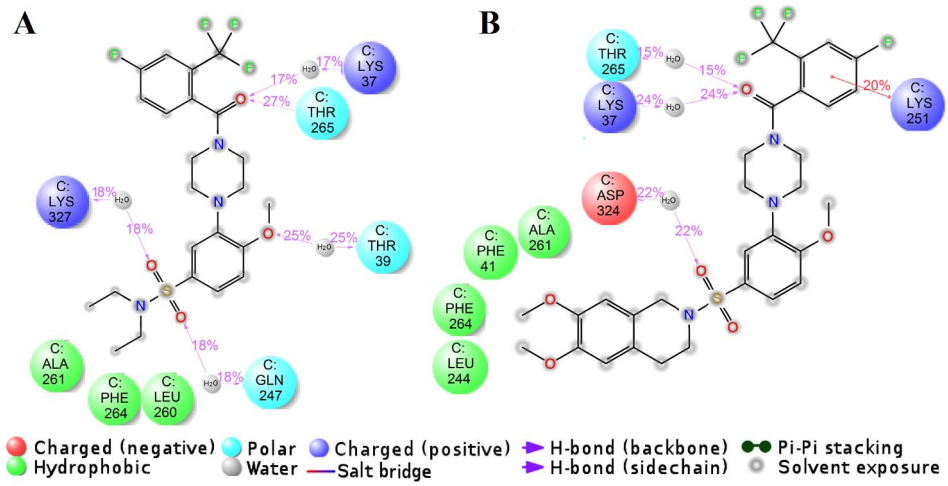

Figure 5. Molecular dynamics calculated protein–ligand contacts at the allosteric site, region C: (A) GFRα1–BT13; (B) GFRα1–BT18. Protein ID: 4UX8.

The MD computed binding modes of compounds BT13 and BT18 at regions A and B of GFRα1 were quite similar to those obtained from the docking calculations and are presented in the Supporting Information of Paper **I** (Figures S2 and S3, respectively).

The binding energy calculations using MM/GBSA method also indicated that the allosteric site at the region C of the GFRα1 structure was preferable for binding both studied ligands, BT13 and BT18. The calculated binding free energy for BT13 was -50.9 kcal/mol, being 3.4 and 2.4 kcal/mol lower as compared to the binding energy for regions A and B, respectively. The calculated binding free energy for ligand BT18 was -55.7 kcal/mol, being 5.0 and 5.9 kcal/mol lower than that for the binding regions A and B (see Table 1 in Paper **I**).

The MD simulations were repeated with another crystal structure of GDNF−GFRα1 complex (PDB ID: 3FUB [120]) for BT13 and BT18. The results obtained were similar for region A, but partly different for region C of the GFRα1 structure. As mentioned above, GFRα1 does not have domain D1 in structure 3FUB, but according to our molecular docking and MD calculations with structure 4UX8, domain D1 may affect the binding of a small-molecule ligand at the allosteric site of GFRα1 (region C). It can be also significant in determining the signalling-related conformational changes.

Additional MD simulations using AMBER package with a different force field were carried out by A. T. García-Sosa in order to verify the binding of BT13 at the allosteric binding site of GFRα1 (see details in Paper **I**). The obtained results were consistent with the Desmond MD results.

In conclusion, our docking calculations and MD simulations demonstrated that the preferable binding of compounds BT13 and BT18 may take place at the allosteric site of GFRα1. The complexes of BT13 and BT18 with GFRα1 were stable throughout several long MD simulation times. As noted above, both studied compounds act experimentally as RET direct agonists. The binding site at RET interface with GFRα1 (region B) probably becomes preferable in the membrane-bound state of RET. This enables BT13 and BT18 to act as direct agonists of RET. However, the computationally predicted binding of the studied compounds to either component of GDNF receptor complex (coreceptor or RET) involves the rather loose and nonspecific hydrophobic and van der Waals interactions and the favoured binding site is rather flat. Therefore, it might not be easy to increase the binding efficiency of the ligands as even minor modifications in the ligand structures can lead to substantial changes in their binding mode and inactivation.

4.1.2. Novel small-molecule ligands as potential GDNF family receptor agonists

In Paper **I**, an allosteric site of GFRα1 was identified as preferable for binding compounds BT13 and BT18. In Paper **II**, a novel potential GFRα1 agonist with a different molecular mechanism of action was designed.

Our analysis of the binding interface between GDNF and GFRα1 using the available crystal structures of the GDNF–GFRα1 complex (PDB ID: 4UX8 [119], 3FUB [120]) enabled to identify the key residues of GFRα1 for interaction with potential small-molecule ligands in the region A of the GFRα1 structure (Figure 2). A potential GFRα1 agonist should be bound in the region of amino acid residues Arg171, Thr179, Arg224, and Gln227, forming hydrogen bonds to Arg171, Arg224 and/or Gln227 (see Figure 2 in Paper **I**). This is in accordance with the previously published data [172,173] on site-directed mutagenesis and mutants. Based on this information, four groups of small-molecule ligands belonging to 10 different scaffolds were examined (Figure 6) using a structure-based drug design (SBDD) approach. All studied compounds were docked in the selected area of GFRα1 (see Table S2 in the Supporting Information of Paper **II**).

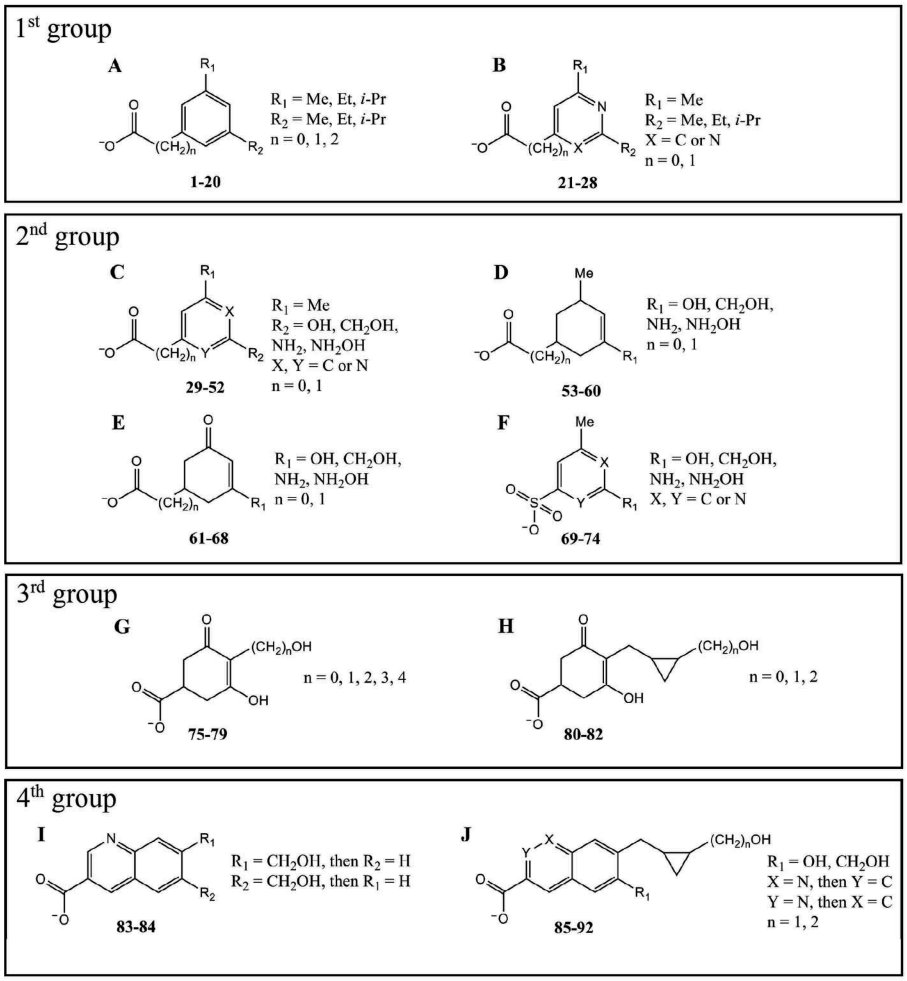

Figure 6. Structures of small-molecule ligands used in the molecular docking to receptor GFRα1.

The first group of compounds consisted of 28 molecules (Figure 6A,B). The calculated binding energies of these ligands were in the range of -4.3 to -5.6 kcal/mol. Only one heterocyclic compound **25** from this group exhibited specific binding to GFRα1 (i.e., a hydrogen bond with the amine group of Arg171, Figure 7A). The second group consisted of 46 structures (Figure 6C-F) with the binding energies ranging between -4.4 to -5.2 kcal/mol. Most of these compounds formed hydrogen bonds with GFRα1 via carboxyl oxygens and/or by the added polar substituent at the R_2 position, by the nitrogen atom of the aromatic cycle, and by an oxygen atom of the sulphonate group (see compound **42** in Figure 7B). The third group of constructed ligands included 8 molecules

with the calculated binding energies in the range of -5.0 to -6.1 kcal/mol. In this group, compound **77** displayed a different binding mode, forming three hydrogen bonds with GFRα1, involving its carboxyl oxygen with the amine group of Arg224, its hydroxypropyl group with the amine group of Gln227, and its hydroxyl group with the carbonyl oxygen of Thr228, respectively (Figure 7C).

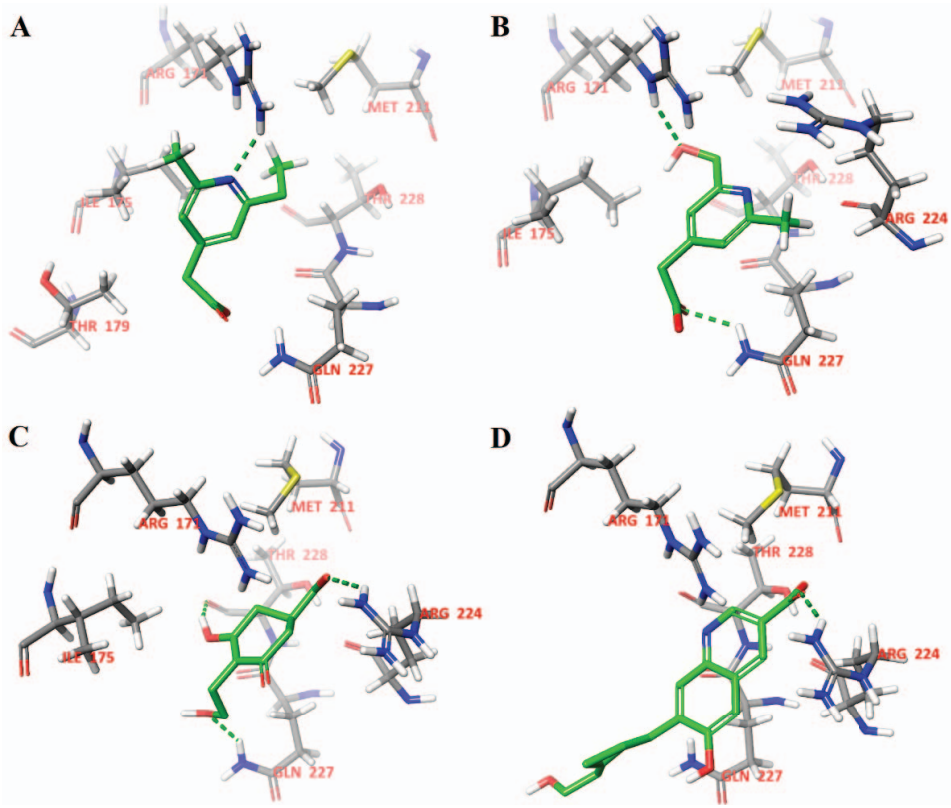

Figure 7. Calculated binding modes of compounds **25** (A), **42** (B), **77** (C), and **86** (D) in the active site of GFRα1. Intermolecular hydrogen bonds are shown by green dashed lines.

The docking results for the first three groups of ligands, indicated that (1) compounds with rigid aromatic ring(s) give lower binding energies than compounds with flexible cycles; (2) hydrogen bonding substituents, such as carboxyl or hydroxyl groups may bind to specific amino acid residues of GFRα1.

The fourth group of ligands was constructed following these indications. This group included 10 compounds (Figure 6I,J). Although the free binding energies of these ligands were the lowest, in the range of -5.5 to -6.4 kcal/mol,

only one hydrogen bond was formed between the carboxyl oxygen atoms of ligands and the amine group of Arg224 residue of GFRα1 (see compound **86** as an example in Figure 7D).

The designed compounds from the last group were used as templates for the similarity search in ZINC [174] and MolPort [175] databases. Five compounds were selected for further biological experiments (Figure 8). The biological experiments were carried out by Y. Sidorova and M. Saarma from Laboratory of Molecular Neuroscience (LMN), Institute of Biotechnology, HiLIFE, University of Helsinki. They found that compounds **107** and **108** activated luciferase by more than 1.5 times using luciferase assay in cells expressing GFRα1–RET [176]. In dose-dependent experiments, compound **107** led to moderate activation of luciferase in 25 μM and 50 μM concentrations, compound **118** demonstrated borderline activation of luciferase in 50 μM concentration.

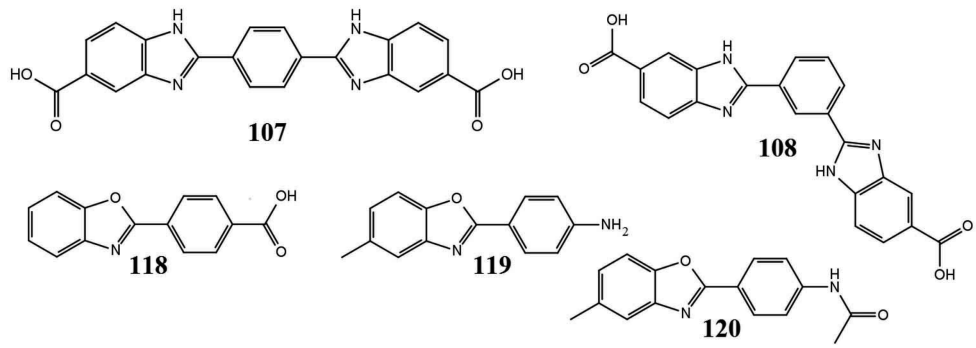

Figure 8. Selected compounds for biological experiments.

The activity of compounds **107** and **118** was also confirmed by RET phosphorylation (pY) assays carried out by LMN in Helsinki using western blotting. Compound **107** activated RET pY in the cells expressing GFRα1–RET but not in the cells expressing only RET. Compound **118** failed to activate RET pY that can be explained by the differences in the sensitivity of assays. According to the experimental results, compound **107**, similarly to GDNF, might require the presence of GFRα1 coreceptor to simulate RET pY. Surprisingly, the meta-substituted compound **108**, the analogue of para-substituted compound **107**, showed no activity in biological experiments. Compounds **119** and **120**, analogues of compound **118**, were also inactive. According to the docking results, all selected compounds had almost the same binding mode in the active centre of GFRα1 (Figure 9). This may indicate that the relative position of the carboxyl group is important for biological activity.

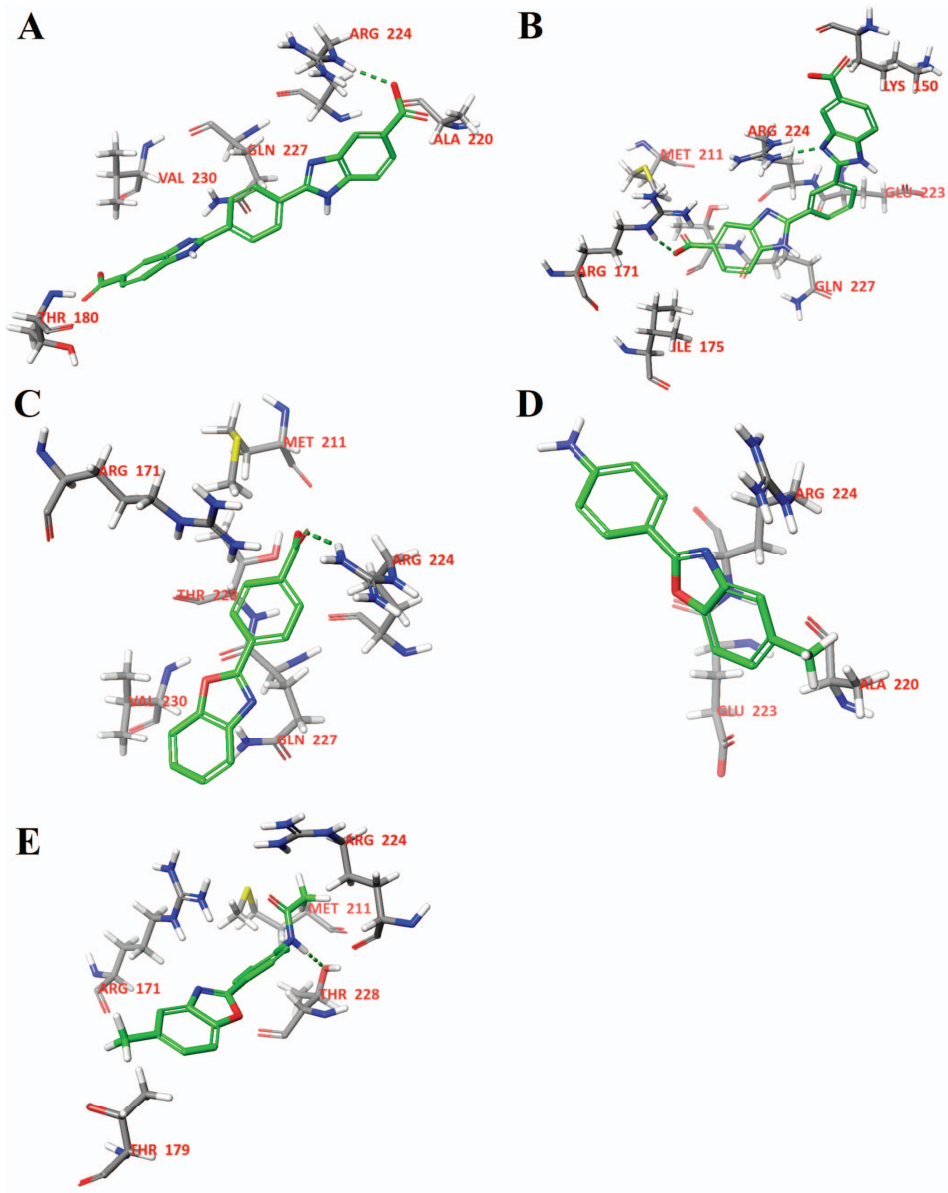

Figure 9. Calculated binding modes of compounds **107** (A), **108** (B), **118** (C), **119** (D), and **120** (E) in the active site of GFRα1. Intermolecular hydrogen bonds are shown by green dashed lines.

The binding mode of compound **107** was also studied by the complementary molecular dynamics modelling. According to the MD results, this compound formed strong hydrogen bonds by its carboxyl groups with Arg224 and Thr228

in the GFRα1 structure. The benzimidazole rings of the ligand were also fixed by the water-assisted interactions with Glu223 and Gln227 in the active site of GFRα1 (Figure 10).

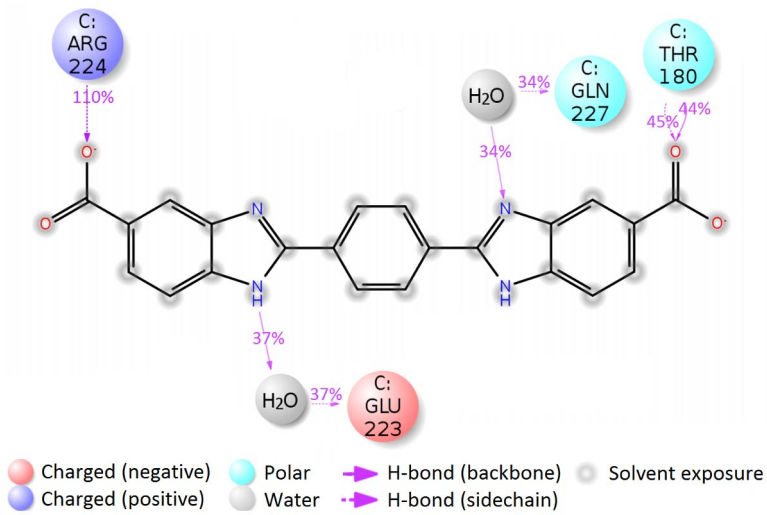

Figure 10. Molecular dynamics calculated binding mode of compound **107**.

Thus, a potential GFRα1 agonist was designed using SBDD and molecular modelling methods. Compound **107** is very different from the earlier reported active compounds XIB4035 [92], BT13 [93], and BT18 [96]. This is not surprising, as it corresponds to a different mechanism of RET activation. Therefore, the 2,2'-(1,4-phenylene)bis-1*H*-benzimidazole backbone of compound **107** can be used as a new scaffold for the development of efficient GFRα1 agonists.

4.2. Combination of QSAR and molecular modelling methods

Molecular modelling and quantitative structure-activity relationship (QSAR) methods are two important computational tools in drug development. Each of them has its advantages and restrictions of application. The molecular docking, virtual screening, and MD simulations are preferably used when the 3D structure of selected protein target is known [177]. The QSAR methods do not have this restriction, but biological experimental data are needed to develop QSAR models and further predictions. The combination of these methods enables to utilize the advantages of both methods. For example, potential inhibitors identified by QSAR prediction models can be used to obtain a highly focused

libraries of compounds. In a similar work by Ambure *et al.* [178], it was showed that a combination of different *in silico* techniques can lead to fast and reliable results.

In Paper **III**, several novel scaffolds for three target proteins – tropomyosin receptor kinase A (TrkA), *N*-methyl-D-aspartate receptor (NMDA), and leucine-rich repeat kinase 2 (LRRK2) – were predicted using the combination of machine learning and molecular modelling methods.

In Paper **IV**, this approach was used to identify potential multitarget compounds, which may act against Alzheimer's disease and simultaneously aim to several protein targets, i.e., acetylcholinesterase (AChE), serotonin transporter (SERT), beta-site amyloid precursor protein cleaving enzyme 1 (BACE1), and glycogen synthase kinase 3 beta (GSK3β). AChE has proven to be the most potent therapeutic target for the symptomatic improvement in Alzheimer's disease, as cholinergic deficit is a consistent and early finding in AD [179]. GSK3β is considered as a critical molecular link between the senile plaques and neurofibrillary tangles two histopathological hallmarks of AD [180]. According to the amyloid cascade hypothesis, BACE1 is also considered as a major therapeutic target in the treatment of neurodegenerative diseases because of the accumulation of Aβ neurotoxic oligomers is a critical molecular event in the pathogenesis of AD [181]. Most publications dealing with the role of serotonin receptors in AD focus on the possible interaction between the serotonergic system and the amyloid-mediated part of pathophysiology, i.e., the interaction is strongly related to the sodium-dependent serotonin transporter (5-HT transporter) [182].

4.2.1. Identification of natural compounds against neurodegenerative diseases using *in silico* techniques

The aim of this study was to identify new potentially active compounds among natural products for three protein targets: TrkA, NMDA, and LRRK2. The studied protein targets are related to various neurodegenerative diseases, such as AD, PD, and neuropathic pain. It has been shown that mutations in LRRK2 are the most common cause of PD [183]. In the case of AD, the synaptic loss, deposition of Aβ plaques, neurofibrillary tangles, and hyperphosphorylated tau are associated with NMDA receptor activation and oxidative stress, which ultimately result in AD pathology [184,185]. Tyrosine kinase receptors play an important role in neuronal survival, together with nerve growth factors associated with AD and intractable pain. Therefore, along with others, the high-affinity receptor TrkA is considered as a target to treat neurodegenerative diseases [186,187].

A subset of natural compounds containing nearly 17,000 compounds (after pre-processing this number was reduced to 13,648) was obtained from ZINC database [174]. The development of QSAR models, virtual screening, and prediction of $\log IC_{50}$ values of the selected compounds was carried out by D. A.

Dobchev (see detailed information in Paper **III**, Sections 2.1, 2.2, and 2.3). The best multilinear regression (BMLR) algorithm and several back-propagation neural network models with different architectures were applied in the development and prediction of QSAR models. The top 100 compounds with the best predicted logIC_{50} by both artificial neural networks (ANN) and BMLR models were selected for further averaged prediction by both models. In result, three sets of compounds for each target were identified. The top 40% of compounds (80 compounds for NMDA and LRRK2 and 40 for TrkA) predicted by the QSAR models for each protein target were further studied using molecular docking. Based on the docking results, three best compounds for each target were selected for further molecular dynamics study. The known inhibitors of NMDA (**GNE-5729**) [188], LRRK2 (**PF-06447475**) [189], and TrkA (**AZ-23**) [190] were used as a positive control. It should be noted that all selected compounds had similar or somewhat smaller binding energies or ligand efficiencies compared to those for the known inhibitors (Table 3). The best selected compounds had also similar binding modes at the active sites of the respective receptors. The binding modes of the selected compounds were confirmed by the results from 50 ns MD simulations. In the case of LRRK2, the stability of MD simulations in time was verified by additional runs of 20, 40, and 60 ns for compound **1L**. The stability of the protein-ligand complexes was evaluated by the RMSD. This parameter varied between 1 and 4 Å for NMDA (except for compound **2N**, which had change at about 35 ns), between 0.8 and 3.6 Å for LRRK2, and between 1 and 4.5 Å for TrkA (Paper **III**).

In the case of NMDA, the binding mode of the ligands to NMDA calculated by molecular dynamics was notably different from that obtained using molecular docking. The binding modes of compound **3N** and the known inhibitor **GNE-5729** (Figure 11A,B) were similar, involving hydrophobic contact with Tyr144, strong water-assisted interaction with the sidechain of Glu132, and strong hydrogen bonding with the backbone of Pro129 residue of the NMDA protein. The binding poses of compounds **1N** and **2N** were also very different, being directed mostly by hydrophobic interactions and water-assisted contacts.

In the case of LRRK2, the contacts of compounds **2L** and **3L** involved strong hydrogen bonds with the amino acid residues of Glu100 and/or Leu102, similarly to the known inhibitor **PF-06447475** (Figure 11C,D). The binding pose of compound **1L** was different, involving two strong hydrogen bonds with Ser34 and Asp162. However, compound **1L** was bound to the active site of LRKK2 and may also act as an inhibitor.

In the case of TrkA, the calculated binding modes of compounds **1T** and **3T** were similar to the binding mode of the known inhibitor **AZ-23**. Both compounds formed strong hydrogen bonds with the backbone of Met592 and long-term hydrophobic contacts with Phe589, Leu657, and Val524 (Figure 11E,F). The binding picture of positively charged compound **2T** was different, forming strong hydrogen bond with Asp668 and specific π–π interaction with the sidechain of Phe589.

Table 3. Calculated binding energies (Δ*G* in kcal/mol) and ligand efficiencies (LE) of small-molecule ligands to receptors (LRRK2, NMDA, and TrkA).

		NMDA		
Compound	**GNE-5729**	**1N**	**2N**	**3N**
Structure	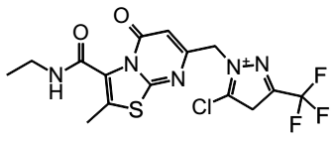	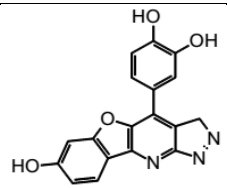	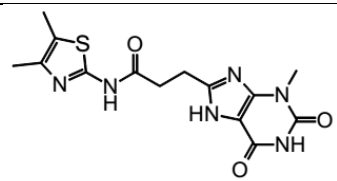	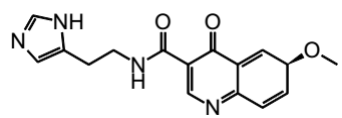
Δ*G*	-11.3	-9.8	-9.7	-9.0
LE	0.42	0.39	0.40	0.39
		LRRK2		
Compound	**PF-06447475**	**1L**	**2L**	**3L**
Structure	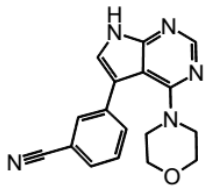	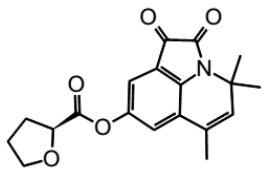	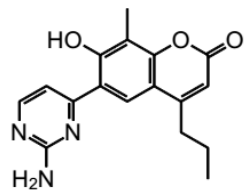	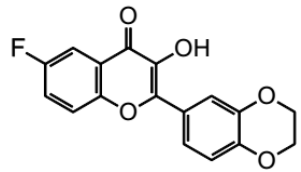
Δ*G*	-9.0	-9.0	-8.5	-8.7
LE	0.39	0.36	0.37	0.38
		TrkA		
Compound	**AZ-23**	**1T**	**2T**	**3T**
Structure	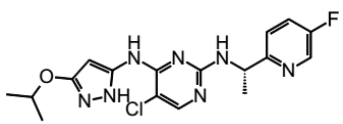	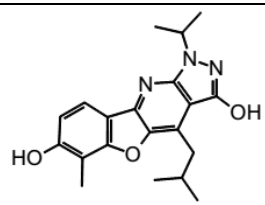	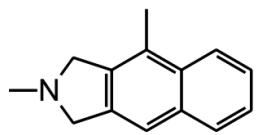	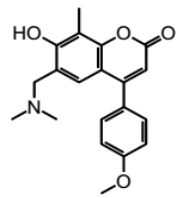
Δ*G*	-8.7	-9.8	-8.6	-9.5
LE	0.32	0.38	0.54	0.38

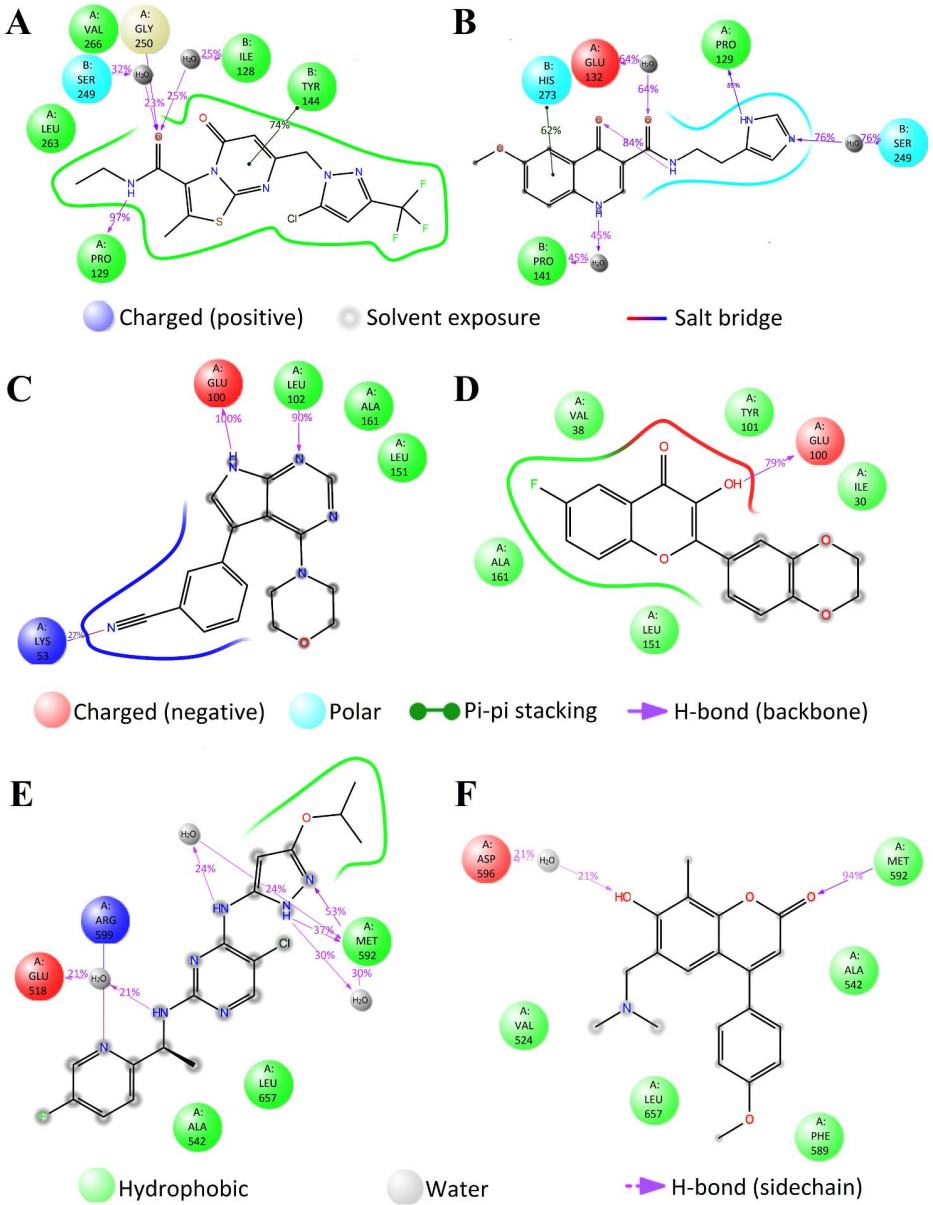

Figure 11. Molecular dynamics calculated contacts between NMDA and **GNE-5729** (A), NMDA and compound **3N** (B), LRRK2 and **PF-06447475** (C), LRRK2 and compound **3L** (D), TrkA and **AZ-23** (E), TrkA and compound **3T** (F).

The interaction energies between the small-molecule ligands and the studied proteins were also estimated using MM/GBSA method [191] (Table 4). The comparison of the MM/GBSA calculated binding energies with those for the

known inhibitors revealed that the NMDA inhibitor **GNE-5279** had significantly better binding energy than any of the newly predicted compounds. However, the ligand efficiency of compound **2N** was sufficiently high and this compound may be of interest as a new potential inhibitor of NMDA. Notably, compound **1L** from the LRRK2 set had significantly better binding energy and ligand efficiency than the known inhibitor **PF-06447475**. Therefore, this compound was predicted as a potential new strong inhibitor of LRRK2. Compound **3L** may also be of interest as a potential LRRK2 inhibitor because its binding energy and ligand efficiency were comparable to those of the known inhibitor. In the case of TrkA, the binding free energy calculations showed that compounds **2T** and **3T** and inhibitor **AZ-23** had close ligand efficiencies. Consequently, these compounds could be tested as potential TrkA inhibitors.

Table 4. Binding free energies (Δ*G* in kcal/mol) and ligand efficiencies (LE) of the complexes between the ligand and NMDA, LRRK2 or TrkA calculated using the MM/GBSA method.

NMDA				
Compound	**GNE-5729**	**1N**	**2N**	**3N**
Δ*G*	-117.25	-78.50	-87.07	-66.39
LE	4.34	3.14	3.63	2.89
LRRK2				
Compound	**PF-06447475**	**1L**	**2L**	**3L**
Δ*G*	-72.41	-100.04	-63.40	-69.12
LE	3.15	4.00	2.76	3.01
TrkA				
Compound	**AZ-23**	**1T**	**2T**	**3T**
Δ*G*	-70.44	-36.13	-43.01	-69.81
LE	2.61	1.39	2.69	2.79

In conclusion, a full cycle *in silico* study involving QSAR modelling, molecular docking, and molecular dynamics simulations enabled us to identify several potential LRRK2, NMDA, and TrkA protein inhibitors. These compounds consist of solid platform for the further development of drug candidates related to neurodegenerative diseases.

4.2.2. Potential multitarget candidates against Alzheimer's disease

The main objective of Paper **IV** was to develop potential candidates for multitarget anti-AD drugs that would be active against four different proteins, namely AChE, BACE1, GSK3β, and SERT. A combination of molecular modelling

(molecular docking, MD simulations), multilinear regression statistical analysis, and ANN methods was used for identification of potential multitarget drug candidates. The general workflow included the following steps:

1. Preparation of the training set for the development of QSAR models and preparation of protein target structures and compounds library;
2. Development of QSAR models;
3. High-throughput virtual screening (HTVS) using molecular docking of biogenic subset of compounds from ZINC database;
4. QSAR prediction of activity of the best binding compounds from HTVS;
5. MD simulations for the best candidates for each of the studied proteins.

The development of QSAR models and prediction of compound activities was carried out by D. A. Dobchev and these results are presented in Paper **IV**, Sections 2.2 and 2.3.

The virtual docking screening was carried out using Vina [136] and Glide HTVS [142,143] programs. Unfortunately, Glide HTVS failed to identify compounds having good binding energy and ligand efficiency for all four or three targets simultaneously. Additional molecular docking with Glide module at extra precision level of the top 60 compounds for each target did not reveal compounds with good binding towards several targets simultaneously and at the same time to satisfy Lipinski's rule (log*P* not greater than 3, not more than 3 hydrogen bond donors, hydrogen bond acceptors, and rotatable bonds) [192]. The virtual screening using Vina allowed to identify 57 compounds with ligand efficiency for each target greater or equal to 0.4. In this set, 22 compounds satisfied all four conditions of Lipinski's rule, the other 35 compounds satisfied at least three of four criteria.

The best binding compounds identified by Vina modelling were selected for further prediction of the biological activity using linear (BMLR) and non-linear (ANN) QSAR models. According to this prediction (see Paper **IV**), 5 compounds (Figure 14) were selected for further experimental testing. The selection of potentially active compounds was based on their binding modes to the target protein as well as their interactions with specific amino acid residues important for the activity of the target protein. The most important amino acid residues of each target protein were identified using the MD simulations of the studied proteins with their known inhibitors. In the case of AChE, these inhibitors were (-)-huperezine A [193], donepezil [193], and (-)-galantamine [194]. The BACE1 inhibitors used in the MD simulations included CNP520 [195], NVP-BXD552 [196], and *N*-{*N*-[4-(acetylamino)-3,5-dichlorobenzyl]carbamimidoyl}-2-(1*H*-indol-1-yl)acetamide (VTI) [197]. In the case of GSK3β, BRD0209 [198], PF-04802367 [199], and *N*-[4-(isoquinolin-7-yl)pyridin-2-yl]cyclopropanecarboxamide (2WF) [200] were studied. The MD simulations with SERT were carried out using the inhibitors paroxetine [201], S-citalopram [202], and sertraline [203].

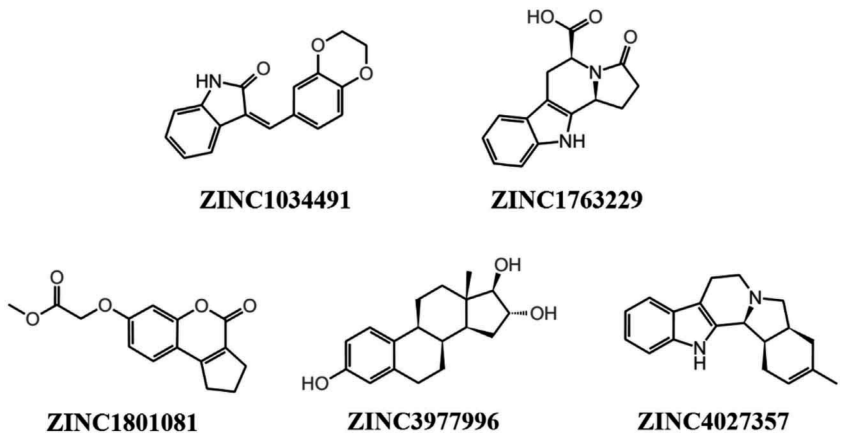

Figure 12. Selected compounds for biological experiments.

According to the molecular docking results, all selected compounds formed specific interactions with at least one key amino acid residue of each target protein. It is worth noting that the selected compounds had the same or even better binding energy/ligand efficiencies as compared to those for the known inhibitors (Table 5).

Table 5. Calculated binding energies (kcal/mol) of the selected small-molecule ligands and the known inhibitors to target proteins (AChE, BACE1, GSK3β, and SERT).

Compound	Binding energy, Δ*G* (kcal/mol)	LE	Compound	Binding energy, Δ*G* (kcal/mol)	LE
AChE			**GSK3β**		
(-)-Huperezine A	-7.9	0.44	**2WF**	-7.1	0.32
(-)-Galantamine	-4.9	0.23	**BRD0209**	-6.9	0.27
Donepezil	-10.2	0.36	**PF-04802367**	-6.9	0.28
ZINC1034491	-9.8	0.47	ZINC1034491	-8.7	0.41
ZINC4027357	-9.3	0.44	ZINC4027357	-8.6	0.41
ZINC3977996	-9.2	0.44	ZINC3977996	-9.1	0.43
ZINC1763229	-9.2	0.46	ZINC1763229	-8.0	0.40
ZINC1801081	-9.1	0.46	ZINC1801081	-8.1	0.41
BACE1			**SERT**		
CNP520	-10.7	0.31	**Paroxetine**	-10.8	0.45
VTI	-9.9	0.34	**S-Citalopram**	-9.5	0.39
NVP-BXD552	-9.2	0.23	**Sertraline**	-9.1	0.46
ZINC1034491	-10.0	0.48	ZINC1034491	-10.3	0.49
ZINC4027357	-10.0	0.48	ZINC4027357	-10.3	0.49
ZINC3977996	-10.2	0.49	ZINC3977996	-10.1	0.48
ZINC1763229	-8.9	0.45	ZINC1763229	-8.9	0.44
ZINC1801081	-9.6	0.48	ZINC1801081	-8.8	0.44

The MD simulations at the active binding site of the studied proteins showed similarity in the binding of the selected compounds to the known inhibitors (**Paper IV**, Section 2.6).

According to the results of QSAR prediction and molecular modelling, compound ZINC3977996 can act as a multitarget inhibitor for all four targets, the other four compounds can act as potential inhibitors for either two or three targets. Specifically, compounds ZINC1034491 and ZINC1801081 can be potential inhibitors for AChE/GSK3β/SERT and compound ZINC4027357 can be a potential inhibitor for AChE/BACE1/SERT. Compound ZINC1763229 can be tested as a potential inhibitor for GSK3β and SERT.

These selected compounds were further tested in the enzyme inhibition assays at concentrations ranging from 0.04 to 25 μM against AChE, BACE1, and GSK3β. Among the predicted potential inhibitors, only compound ZINC4027357 exhibited significant activity against two studied proteins, AChE and BACE1 (IC_{50} = 0.55 μM and 5.2 μM, respectively). Compounds ZINC1801081 and ZINC3977996 showed moderate inhibitory activity against AChE at a concentration greater than 20 μM.

Thus, a combination of different QSAR methods and molecular modelling allowed to identify a new potential multitarget agent against two proteins associated with Alzheimer's disease that would be valuable starting compound in further development of multitarget drugs against Alzheimer's disease.

SUMMARY

The main objective of the current thesis was to identify and develop active compounds against the biological targets related to neurodegenerative diseases and to study their mechanism of the action using different molecular modelling methods. The basic tools used in this work were high-throughput virtual screening based on molecular docking and molecular dynamics simulations.

The first part of this work involved a detailed study of the mechanism of interaction and binding between glial cell line-derived neurotrophic factor (GDNF) family receptor GFRα1 and its previously discovered BT13 and BT18 agonists as well as the development of small molecules that mimic the effects of GDNF. GDNF binds to GFRα1 and then this complex binds to transmembrane receptor tyrosine kinase RET triggering intracellular signalling. In **Paper I**, the mechanism of action of the known agonists BT13 and BT18 on the protein GFRα1 was studied using molecular docking and molecular dynamics simulation approaches. An allosteric site was identified in GFRα1 as preferential for the binding of these ligands. However, considering that the studied compounds have been shown experimentally to be direct GDNF signalling receptor RET agonists, it can be assumed that the binding site at the RET interface with GFRα1 becomes preferable in the membrane-bound state of RET. In this case, these compounds are enabled to act as direct agonists. Nevertheless, this elucidation of the detailed mechanism of interaction between the known active ligands and the GFRα1 and RET receptor complex enables further rational design of highly effective GDNF mimicking small molecules. The structure-based drug design approach was successfully applied in **Paper II** to find out a new potential GDNF family receptor agonist with a different mechanism of RET activation. Despite its moderate biological activity according to the experimental measurements, it is the first compound directly activating GDNF receptor RET via GFRα1 coreceptor in the absence of endogenous neurotrophic factor, which makes it more selective than the previously described compounds BT13 and BT18.

The second part of this study focused on the application of a combination of QSAR and molecular modelling methods in the development of new drug candidates against neurodegenerative disorders. In **Paper III**, a subset of natural compounds was passed through a full cycle of an *in silico* study. As a result, several new scaffolds of the compounds were detected for protein targets NMDA, LRRK2, and TrkA related to Alzheimer's disease, Parkinson's disease, and neuropathic pain, respectively. A combination of different QSAR methods and molecular modelling as well as experimental measurements were applied in **Paper IV** to search active inhibitors against protein targets AChE, SERT, BACE1, and GSK3β that are related to Alzheimer's disease. A new potential multitarget agent against two protein targets (AChE and BACE1) with activity in the micromolar range was identified. The chemical modifications of all

identified compounds could lead to novel drug candidates against the studied protein targets.

In conclusion, eight protein targets related to several neurodegenerative diseases were studied. The discovered novel active compounds belonging to different chemical scaffolds can serve as a basis for the further development of drugs for the treatment of neurodegenerative diseases as well as for a deeper understanding of the pathogenesis and the mechanisms of the development of these disorders.

REFERENCES

1. WHO. The epidemiology and impact of dementia: current state and future trends. Geneva: World Health Organization; **2015**, Document WHO/MSD/MER/ 15.3, available at http://www.who.int/mental_health/neurology/dementia/dementia_ thematicbrief_epidemiology.pdf (accessed 09 January 2020).
2. Prince, M., Wimo, A., Guerchet, M., Ali, G.S., Wu, Y.-T., Prina, M. World Alzheimer Report 2015. The global impact of dementia: an analysis of prevalence. Incidence, cost and trends. London: Alzheimer's Disease International; **2015**.
3. Global Health Estimates 2016: Deaths by Cause, Age, Sex, by Country and by Region, 2000–2016, Geneva, World Health Organization; **2016**.
4. Chen, H., Burton, E.A., Ross, G.W., Huang, X., Savica, R., Abbott, R.D., *et al.* Research on the premotor symptoms of Parkinson's disease: clinical and etiological implications. *Environ. Health Perspect.* **2013**, 121(11–12), 1245–1252.
5. WHO, https://www.who.int/news-room/fact-sheets/detail/dementia (accessed online 30-Apr-2020).
6. Zeng, H., Wu, X. Alzheimer's disease drug development based on computer-aided drug design. Eur. *J. Med. Chem.* **2016**, 121, 851–863.
7. Baig, M.H., Ahmad, K., Rabbani, G., Danishuddin, M., Choi, I. Computer aided drug design and its application to the development of potential drugs for neurodegenerative disorders. *Curr. Neuropharmacol*. **2018**, 16(6), 740–748.
8. Durães, F., Pinto, M., Sousa, E. Old Drugs as New Treatments for Neurodegenerative Diseases. *Pharmaceuticals (Basel)* **2018**, 11(2), pii: E44.
9. Smith, Y., Wichmann, T., Factor, S.A., DeLong, M.R. Parkinson's disease therapeutics: new developments and challenges since the introduction of levodopa. *Neuropsychopharmacology* **2012**, 37(1), 213–246.
10. Danon, J.J., Reekie, T.A., Kassiou, M. Challenges and opportunities in central nervous system drug discovery. *Trends in Chem*. **2019**, 1(6), 612–624.
11. Jntu, K.V.R., Jntu, L.P.R. A neural network-based classification and diagnosis of brain hemorrhages. In Allied Academies International Conference. Academy of Information and Management Sciences. Proceedings, Jordan Whitney Enterprises, Inc, **2009**, 13, 52.
12. Lin, J.S. Brain structures and mechanisms involved in the control of cortical activation and wakefulness, with emphasis on the posterior hypothalamus and histaminergic neurons. *Sleep. Med. Rev*. **2000**, 4(5), 471–503.
13. Navarrete, A., van Schaik, C.P., Isler, K. Energetics and the evolution of human brain size. *Nature* **2011**, 480(7375), 91–93.
14. Sehgal, S.A., Hammad, M.A., Tahir, R.A., Akram, H.N., Ahmad, F. Current therapeutic molecules and targets in neurodegenerative diseases based on in silico drug design. *Curr. Neuropharmacol*. **2018**, 16(6), 649–663.
15. Geula, C., Mesulam, M.M. Cholinesterases and the pathology of Alzheimer disease. *Alzheimer Dis. Assoc. Disord*. **1995**, 9(2), 23–28.
16. Varadaraju, K.R., Kumar, J.R., Mallesha, L., Muruli, A., Mohana, K.N., Mukunda, C.K., *et al*. Virtual screening and biological evaluation of piperazine derivatives as human acetylcholinesterase inhibitors. *Int. J. Alzheimers Dis*. **2013**, 2013:653962.
17. Perry, E., Perry, R., Blessed, G., Tomlinson, B. Necropsy evidence of central cholinergic deficits in senile dementia. *The Lancet* **1977**, 309, 189.
18. Wang, R., Reddy, P.H. Role of Glutamate and NMDA Receptors in Alzheimer's Disease. *J. Alzheimers Dis.* **2017**, 57(4), 1041–1048.

19. Fukumoto, H., Cheung, B.S., Hyman, B.T., Irizarry, M.C. β-Secretase protein and activity are increased in the neocortex in Alzheimer disease. *Archives of Neurology* **2002**, 59, 1381–1389.
20. Vassar, R., Bennett, B.D., Babu-Khan, S., Kahn, S., Mendiaz, E.A., Denis, P., *et al*. β-Secretase Cleavage of Alzheimer's Amyloid Precursor Protein by the Transmembrane Aspartic Protease BACE. *Science* **1999**, 286, 735–741.
21. Rodríguez, J.J., Noristani, H.N., Verkhratsky, A. The serotonergic system in ageing and Alzheimer's disease. *Progr. Neurobiol*. **2012**, 99, 15–41.
22. Llorens-Martín, M., Jurado, J., Hernández, F., Avila, J. GSK-3β, a pivotal kinase in Alzheimer disease. *Front. Mol. Neurosci*. **2014**, 7, 46.
23. Jiang, S., Li, Y., Zhang, C., Zhao, Y., Bu, G., Xu, H., *et al*. M1 muscarinic acetylcholine receptor in Alzheimer's disease. *Neurosci. Bull.* **2014**, 30(2), 295–307.
24. Brown, M.S., Ye, J., Rawson, R.B., Goldstein, J.L. Regulated intramembrane proteolysis: a control mechanism conserved from bacteria to humans. *Cell* **2000**, 100, 391–398.
25. Krishnaswamy, S., Verdile, G., Groth, D., Kanyenda, L., Martins, R.N. The structure and function of Alzheimer's gamma secretase enzyme complex. *Crit. Rev. Clin. Lab. Sci.* **2009**, 46, 282–301.
26. Grooms, S.Y., Opitz, T., Bennett, M.V., Zukin, R.S. Status epilepticus decreases glutamate receptor 2 mRNA and protein expression in hippocampal pyramidal cells before neuronal death. *Proc. Natl. Acad. Sci. USA* **2000**, 97, 3631–3636.
27. Kwak, S., Weiss, J.H. Calcium-permeable AMPA channels in neurodegenerative disease and ischemia. *Curr. Opin. Neurobiol*. **2006**, 16, 281–287.
28. Ray, S., Liu, M. Current understanding of LRRK2 in Parkinson's disease: biochemical and structural features and inhibitor design. *Future Med. Chem.* **2012**, 4(13), 1701–1713.
29. Siddiqui, I.J., Pervaiz, N., Abbasi, A.A. The Parkinson disease gene SNCA: Evolutionary and structural insights with pathological implication. *Sci. Rep.* **2016**, 6, 24475.
30. Cardona, F., Sánchez-Mut, J.V., Dopazo, H., Pérez-Tur, J. Phylogenetic and in silico structural analysis of the Parkinson disease related kinase PINK1. *Hum. Mutat.* **2011**, 32(4), 369–378.
31. Ansari, M.Z. Computational approach towards targeting aggregate formation in Synucleinopathies. *Proteom. Bioinform*. **2015**, 2(6), 181–184.
32. Valentine, J.S., Doucette, P.A., Zittin Potter, S. Copper-zinc superoxide dismutase and amyotrophic lateral sclerosis. *Annu. Rev. Biochem*. **2005**, 74, 563–593.
33. Huang, H.J., Chang, T.T, Chen, H.Y., Chen, C.Y.C. Finding inhibitors of mutant superoxide dismutase-1 for amyotrophic lateral sclerosis therapy from traditional chinese medicine. *Evid. Based Complement. Alternat. Med.* **2014**, 2014:156276.
34. Pasinelli, P., Houseweart, M.K., Brown, R.H. Jr., Cleveland, D.W. Caspase-1 and 3 are sequentially activated in motor neuron death in Cu, Zn superoxide dismutase-mediated familial amyotrophic lateral sclerosis. *Proc. Natl. Acad. Sci. USA* **2000**, 97(25), 13901–13906.
35. Makhouri, F.R., Ghasemi, J.B. High-throughput docking and molecular dynamics simulations towards the identification of novel peptidomimetic inhibitors against CDC7. *Mol. Inf.* **2018**, 37, e1800022.
36. Bendotti, C., Atzori, C., Piva, R., Tortarolo, M., Strong, M.J., DeBiasi, S., *et al*. Activated p38MAPK is a novel component of the intracellular inclusions found in

human amyotrophic lateral sclerosis and mutant SOD1 transgenic mice. *J. Neuropathol. Exp. Neurol.* **2004**, 63, 113–119.
37. Sierra Bello, O., Gonzalez, J., Capani, F., Barreto, G.E. In silico docking reveals possible Riluzole binding sites on Nav1.6 sodium channel: implications for amyotrophic lateral sclerosis therapy. *J. Theor. Biol*. **2012**, 315, 53–63.
38. Bhattacharyya, N.P., Banerjee, M., Majumder, P. Huntington's disease: roles of huntingtin-interacting protein 1 (HIP-1) and its molecular partner HIPPI in the regulation of apoptosis and transcription. *FEBS J*. **2008**, 275(17), 4271–4279.
39. Fan, J., Cowan, C.M., Zhang, L.Y., Hayden, M.R., Raymond, L.A. Interaction of postsynaptic density protein-95 with NMDA receptors influences excitotoxicity in the yeast artificial chromosome mouse model of Huntington's disease. *J. Neurosci.* **2009**, 29(35), 10928–10938.
40. Li, X., Sapp, E., Valencia, A., Kegel, K.B., Qin, Z.H., Alexander, J., *et al*. A function of huntingtin in guanine nucleotide exchange on Rab11. *Neuroreport.* **2008**, 19(16), 1643–1647.
41. Bothwell, M. Recent advances in understanding neurotrophin signaling. *F1000Res*. **2016**, 5, 1885.
42. Bothwell, M. NGF, BDNF, NT3, and NT4. *Handb. Exp. Pharmacol*. **2014**, 220, 3–15.
43. Ibáñez, C.F., Andressoo, J.O. Biology of GDNF and its receptors - relevance for disorders of the central nervous system. *Neurobiol. Dis*. **2017**, 97, 80–89.
44. Kerschensteiner, M., Stadelmann, C., Dechant, G., Wekerle, H., Hohlfeld, R. Neurotrophic cross-talk between the nervous and immune systems: Implications for neurological diseases. *Ann. Neurol*. **2003**, 53, 292–304.
45. Lindahl, M., Saarma, M., Lindholm, P. Unconventional neurotrophic factors CDNF and MANF: Structure, physiological functions and therapeutic potential. *Neurobiol. Dis.* **2017**, 97, 90–102.
46. Sidorova, Y.A., Saarma, M. Glial cell line-derived neurotrophic factor family ligands and their therapeutic potential. *Mol. Biol.* **2016**, 50, 521–531.
47. Thoenen, H., Sendtner, M. Neurotrophins: from enthusiastic expectations through sobering experiences to rational therapeutic approaches. *Nat. Neurosci.* **2002**, 5, 1046–1050.
48. Saragovi, H.U., Galan, A., Levin, L.A. Neuroprotection: pro-survival and anti-neurotoxic mechanisms as therapeutic strategies in neurodegeneration. *Front. Cell Neurosci.* **2019**, 13, 231.
49. Lin, L.F., Doherty, D.H., Lile, J.D., Bektesh, S., Collins, F. GDNF: A glial cell line-derived neurotrophic factor for midbrain dopaminergic neurons. *Science* **1993**, 260, 1130–1132.
50. Treanor, J.J., Goodman, L., de Sauvage, F., Stone, D.M., Poulsen, K.T., Beck, C.D., *et al*. Characterization of a multicomponent receptor for GDNF. *Nature* **1996**, 382(6586), 80–83.
51. Airaksinen, M.S., Saarma, M. The GDNF family: signalling, biological functions and therapeutic value. *Nat. Rev. Neurosci*. **2002**, 3, 383–394.
52. Lin, L.F., Doherty, D.H., Lile, J.D., Bektesh, S., Collins, F. GDNF: A glial cell line-derived neurotrophic factor for midbrain dopaminergic neurones. *Science* **1993**, 260, 1130–1132.
53. Eigenbrot, C., Gerber, N. X-ray structure of glial cell derived neurotrophic factor at 1.9 A resolution and implications for receptor binding. *Nat. Struct. Biol.* **1997**, 4, 435–438.

54. Meng, X., de Rooij, D.G., Westerdahl, K., Saarma, M., Sariola, H. Promotion of seminomatous tumors by targeted over expression of glial cell line-derived neurotrophic factor in mouse testis. *Cancer Res.* **2001**, 61, 3267–3271.
55. Tomac, A., Lindqvist, E., Lin, L.F.H., Ogren, S.O., Young, D., Hoffer, B.J., *et al*. Protection and repair of the nigrostriatal dopaminergic system by GDNF in vivo. *Nature* **1995**, 373, 335–339.
56. Gash, D.M., Zhang, Z., Ovadia, A., Cass, W.A., Yi, A., Simmerman, L., *et al*. Functional recovery in parkinsonian monkeys treated with GDNF. *Nature* **1996**, 380, 252–255.
57. Björklund, A., Rosenblad, C., Winkler, C., Kirik, D. Studies on neuroprotective and regenerative effects of GDNF in a partial lesion model of Parkinson's disease. *Neurobiol. Dis.* **1997**, 4, 186–200.
58. Choi-Lundberg, D.L., Lin, Q., Chang, Y.N., Chiang, Y.L., Hay, C.M., Mohajeri, H., *et al*. Dopaminergic neurons protected from degeneration by GDNF gene therapy. *Science* **1997**, 275, 838–841.
59. Grondin, R., Zhang, Z., Yi, A., Cass, W.A., Maswood, N., Andersen, A.H., *et al*. Chronic, controlled GDNF infusion promotes structural and functional recovery in advanced parkinsonian monkeys. *Brain* **2002**, 125, 2191–2201.
60. Mohajeri, M.H., Figlewicz, D.A., Bohn, M.C. Intramuscular grafts of myoblasts genetically modified to secrete glial cell line-derived neurotrophic factor prevent motoneuron loss and disease progression in a mouse model of familial amyotrophic lateral sclerosis (FALS). *Human Gene Therapy* **1999**, 10, 1853–1866.
61. Forlenza, O.V., Miranda, A.S., Guimar, I., Talib, L.L., Diniz, B.S., Gattaz, W.F., *et al*. Decreased Neurotrophic Support is Associated with Cognitive Decline in Non-Demented Subjects. *J. Alzheimers Dis.* **2015**, 46(2), 423–429.
62. Ghribi, O., Herman, M.M., Forbes, M.S., DeWitt, D.A., Savory, J. GDNF protects against aluminum-induced apoptosis in rabbits by upregulating Bcl-2 and Bcl-XL and inhibiting mitochondrial Bax translocation. *Neurobiol. Dis.* **2001**, 8(5), 764–773.
63. Pertusa, M., García-Matas, S., Mammeri, H., Adell, A., Rodrigo, T., Mallet, J., *et al*. Expression of GDNF transgene in astrocytes improves cognitive deficits in aged rats. *Neurobiol. Aging* **2008**, 29(9), 1366–1379.
64. Grondin, R., Cass, W.A., Zhang, Z., Stanford, J.A., Gash, D.M., Gerhardt, G.A. Glial cell line-derived neurotrophic factor increases stimulus-evoked dopamine release and motor speed in aged rhesus monkeys. *J. Neurosci.* **2003**, 23(5), 1974–1980.
65. Gill, S.S., Patel, N.K., Hotton, G.R., O'Sullivan, K., McCarter, R., Bunnage, M., *et al*. Direct brain infusion of glial cell line-derived neurotrophic factor in Parkinson disease. *Nat. Med.* **2003**, 9, 589–595.
66. Kirik, D., Georgievska, B., Bjorklund, A. Localized striatal delivery of GDNF as a treatment for Parkinson disease. *Nat. Neurosci.* **2004**, 7, 105–110.
67. Marks, W.J. Jr., Bartus, R.T., Siffert, J., Davis, C.S., Lozano, A., Boulis, N., *et al*. Gene delivery of AAV2-neurturin for Parkinson's disease: a double-blind, randomised, controlled trial. *Lancet Neurol*. **2010**, 9, 1164–1172.
68. LeSauteur, L., Wei, L., Gibbs, B.F., Saragovi, H.U. Small peptide mimics of nerve growth factor bind TrkA receptors and affect biological responses. *J. Biol. Chem.* **1995**, 270, 6564–6569.

69. LeSauteur, L., Cheung, N.K., Lisbona, R., Saragovi, H.U. Small molecule nerve growth factor analogs image receptors in vivo. *Nat. Biotechnol.* **1996**, 14, 1120–1122.
70. Debeir, T., Saragovi, H.U., Cuello, A.C. A nerve growth factor mimetic TrkA antagonist causes withdrawal of cortical cholinergic boutons in the adult rat. *PNAS U.S.A.* **1999,** 96, 4067–4072.
71. Maliartchouk, S., Debeir, T., Beglova, N., Cuello, A.C., Gehring, K., Saragovi, H.U. Genuine monovalent ligands of TrkA nerve growth factor receptors reveal a novel pharmacological mechanism of action. *J. Biol. Chem.* **2000**, 275, 9946–9956.
72. Maliartchouk, S., Feng, Y., Ivanisevic, L., Debeir, T., Cuello, A.C., Burgess, K., *et al*. A designed peptidomimetic agonistic ligand of TrkA nerve growth factor-receptors. *Mol. Pharmacol.* **2000**, 57, 385–391.
73. Pattarawarapan, M., Zaccaro, M.C., Saragovi, U.H., Burgess, K. New templites for syntheses of ring-fused, C(10) beta-turn peptidomimetics leading to the first reported small-molecule mimic of neurotrophin-3. *J. Med. Chem.* **2002**, 45, 4387–4390.
74. Zaccaro, M.C., Lee, H.B., Pattarawarapan, M., Xia, Z., Caron, A., L'Heureux, P.J., *et al.* Selective small molecule peptidomimetic ligands of TrkC and TrkA receptors afford discrete or complete neurotrophic activities. *Chem. Biol.* **2005**, 12, 1015–1028.
75. Chen, D., Brahimi, F., Angell, Y., Li, Y.C., Moscowicz, J., Saragovi, H.U., *et al*. Bivalent peptidomimetic ligands of TrkC are biased agonists and selectively induce neuritogenesis or potentiate neurotrophin-3 trophic signals. *ACS Chem. Biol*. **2009**, 4, 769–781.
76. LeSauteur, L., Maliartchouk, S., Le Jeune, H., Quirion, R., Saragovi, H.U. Potent human p140-TrkA agonists derived from an anti-receptor monoclonal antibody. *J. Neurosci.* **1996**, 16, 1308–1316.
77. Saragovi, H.U., Zheng, W., Maliartchouk, S., DiGugliemo, G.M., Mawal, Y.R., Kamen, A., *et al.* A TrkA-selective, fast internalizing nerve growth factor-antibody complex induces trophic but not neuritogenic signals. *Biol. J. Chem.* **1998**, 273, 34933–34940.
78. Bai, Y., Xu, J., Brahimi, F., Zhuo, Y., Sarunic, M.V., Saragovi, H.U., *et al.* An agonistic anti-TrkB mAb, but not BDNF, causes sustained TrkB activation, delays RGC death, and protects the retinal structure in optic nerve axotomy and in glaucoma. *Invest. Ophthalmol. Vis. Sci.* **2010**, 51, 4722–4731.
79. Guillemard, V., Ivanisevic, L., Garcia, A.G., Scholten, V., Lazo, O.M., Bronfman, F.C., *et al.* An agonistic mAb directed to the TrkC receptor juxtamembrane region defines a trophic hot spot and interactions with p75 coreceptors. *Dev. Neurobiol.* **2010**, 70, 150–164.
80. Brahimi, F., Malakhov, A., Lee, H.B., Pattarawarapan, M., Ivanisevic, L., Burgess, K., *et al.* A peptidomimetic of NT-3 acts as a TrkC antagonist. *Peptides* **2009**, 30, 1833–1839.
81. Brahimi, F., Liu, J., Malakhov, A., Chowdhury, S., Purisima, E.O., Ivanisevic, L. *et al.* A monovalent agonist of TrkA tyrosine kinase receptors can be converted into a bivalent antagonist. *Biochim. Biophys. Acta* **2010**, 1800(9), 1018–1026.
82. Brahimi, F., Ko, E., Malakhov, A., Burgess, K., Saragovi, H.U. Combinatorial assembly of small molecules into bivalent antagonists of TrkC or TrkA receptors. *PLoS One* **2014**, 9:e89617.

83. Berezov, A., Chen, J., Liu, Q., Zhang, H.T., Greene, M.I., Murali, R., *et al*. Disabling receptor ensembles with rationally designed interface peptidomimetics. *J. Biol. Chem.* **2002**, 277, 28330–28339.
84. Jang, S.W., Liu, X., Yepes, M., Shepherd, K.R., Miller, G.W., Liu, Y., *et al*. A selective TrkB agonist with potent neurotrophic activities by 7,8 dihydroxyflavone. *PNAS U.S.A.* **2010**, 107, 2687–2692.
85. Devi, L, Ohno, M. 7,8-dihydroxyflavone, a small-molecule TrkB agonist, reverses memory deficits and BACE1 elevation in a mouse model of Alzheimer's disease. *Neuropsychopharmacology* **2012**, 37, 434–444.
86. Bollen, E., Vanmierlo, T., Akkerman, S., Wouters, C., Steinbusch, H.M., Prickaerts, J., *et al*. 7,8-Dihydroxyflavone improves memory consolidation processes in rats and mice. *Behav. Brain Res.* **2013**, 257, 8–12.
87. Coles, C.H., Mitakidis, N., Zhang, P., Elegheert, J., Lu, W., Stoker, A.W., *et al.* Structural basis for extracellular cis and trans RPTP sigma signal competition in synaptogenesis. *Nat. Commun*. **2014**, 5, 5209.
88. Chitranshi, N., Gupta, V., Kumar, S., Graham, S.L. Exploring the molecular interactions of 7,8-dihydroxyflavone and its derivatives with TrkB and VEGFR2 proteins. *Int. J. Mol. Sci*. **2015**, 16, 21087–21108.
89. Nie, S., Xu, Y., Chen, G., Ma, K., Han, C., Guo, Z., *et al.* Small molecule TrkB agonist deoxygedunin protects nigrostriatal dopaminergic neurons from 6-OHDA and MPTP induced neurotoxicity in rodents. *Neuropharmacology* **2015**, 99, 448–458.
90. Jiang, M., Peng, Q., Liu, X., Jin, J., Hou, Z., Zhang, J., *et al.* Small molecule TrkB receptor agonists improve motor function and extend survival in a mouse model of Huntington's disease. *Hum. Mol. Genet.* **2013**, 22, 2462–2470.
91. Simmons, D.A., Belichenko, N.P., Yang, T., Condon, C., Monbureau, M., Shamloo, M., *et al.* A small molecule TrkB ligand reduces motor impairment and neuropathology in R6/2 and BACHD mouse models of Huntington's disease. *J. Neurosci.* **2013**, 33, 18712–18727.
92. Tokugawa, K., Yamamoto, K., Nishiguchi, M., Sekine, T., Sakai, M., Ueki, T., *et al*. XIB4035, a novel nonpeptidyl small molecule agonist for GFRα-1. *Neurochem. Int.* **2003**, 42, 81−86.
93. Sidorova, Y.A., Bespalov, M.M., Wong, A.W., Kambur, O., Jokinen, V., Lilius, T.O., *et al*. A Novel Small Molecule GDNF Receptor RET Agonist, BT13, Promotes Neurite Growth from Sensory Neurons in Vitro and Attenuates Experimental Neuropathy in the Rat. *Front. Pharmacol.* **2017**, 8, 365.
94. Hedstrom, K.L., Murtie, J.C., Albers, K., Calcutt, N.A., Corfas, G. Treating small fiber neuropathy by topical application of a small molecule modulator of ligand induced GFRalpha/RET receptor signaling. *PNAS U.S.A.* **2014**, 111, 2325–2330.
95. Doonan, F., O'Driscoll, C., Kenna, P., Cotter, T.G. Enhancing survival of photoreceptor cells in vivo using the synthetic progestin Norgestrel. *J. Neurochem.* **2011**, 118, 915–927.
96. Bespalov, M.M., Sidorova, Y.A., Suleymanova, I., Thompson, J., Kambur, O., Jokinen, V., *et al*. Novel agonist of GDNF family ligand receptor RET for the treatment of experimental neuropathy. **2016**, *bioRxiv*: 061820.
97. Sidorova, Y.A., Volcho, K.P., Salakhutdinov, N.F. Neuroregeneration in Parkinson's Disease: From Proteins to Small Molecules. *Curr. Neuropharmacol.* **2019**, 17(3), 268–287.

98. Wong, D.F., Rosenberg, P.B., Zhou, Y., Kumar, A., Raymont, V., Ravert, H.T., *et al*. In Vivo Imaging of Amyloid Deposition in Alzheimer Disease Using the Radioligand 18F-AV-45 (Flobetapir F 18). *J. Nucl. Med.* **2010**, 51(6), 913–920.
99. Olabarria, M., Noristani, H.N., Verkhratsky, A., Rodríguez, J.J. Concomitant astroglial atrophy and astrogliosis in a triple transgenic animal model of Alzheimer's disease. *Glia* **2010**, 58, 831–838.
100. Jin, M., Shepardson, N., Yang, T., Chen, G., Walsh, D., Selkoe, D.J. Soluble amyloid β-protein dimers isolated from Alzheimer cortex directly induce Tau hyperphosphorylation and neuritic degeneration. *PNAS U. S. A.* **2011**, 108, 5819–5824.
101. Wang, J.-Z., Tung, Y.C., Wang, Y., Li, X.T., Iqbal, K., Grundke-Iqbal, I. Hyperphosphorylation and accumulation of neurofilament proteins in Alzheimer disease brain and in okadaic acid-treated SY5Y cells. *FEBS Lett*. **2001**, 507, 81–87.
102. Heredia, L., Helguera, P., de Olmos, S., Kedikian, G., Vigo, F.S., LaFerla, F., *et al*. Phosphorylation of actin-depolymerizing factor/cofilin by LIM-kinase mediates amyloid β-induced degeneration: a potential mechanism of neuronal dystrophy in Alzheimer's disease. *J. Neurosci.* **2006**, 26, 6533–6542.
103. Praticò, D. Evidence of oxidative stress in Alzheimer's disease brain and antioxidant therapy. *Ann. N. Y. Acad. Sci.* **2008**, 1147, 70–78.
104. Kumar, A., Nisha, C.M., Silakari, C., Sharma, I., Anusha, K., Gupta, N., *et al*. Current and novel therapeutic molecules and targets in Alzheimer's disease. *J. Formos. Med. Assoc*. **2016**, 115, 3–10.
105. Ibrahim, M.M., Gabr, M.T. Multitarget therapeutic strategies for Alzheimer's disease. *Neural. Regen. Res.* **2019**, 14(3), 437–440.
106. Sharma, P., Tripathi, A., Tripathi, P.N., Prajapati, S.K., Seth, A., Tripathi, M.K., *et al*. Design and development of multitarget-directed N-Benzylpiperidine analogs as potential candidates for the treatment of Alzheimer's disease. *Eur. J. Med. Chem.* **2019**, 167, 510–524.
107. Cong, L., Dong, X., Wang, Y., Deng, Y., Li, B., Dai, R. On the role of synthesized hydroxylated chalcones as dual functional amyloid-β aggregation and ferroptosis inhibitors for potential treatment of Alzheimer's disease. *Eur. J. Med. Chem.* **2019**, 166, 11–21.
108. Fang, Y., Zhou, H., Gu, Q., Xu, J. Synthesis and evaluation of tetrahydroisoquinoline-benzimidazole hybrids as multifunctional agents for the treatment of Alzheimer's disease. *Eur. J. Med. Chem.* **2019**, 167, 133–145.
109. González-Naranjo, P., Pérez-Macias, N., Pérez, C., Roca, C., Vaca, G., Girón, R., *et al*. Indazolylketones as new multitarget cannabinoid drugs. *Eur. J. Med. Chem*. **2019**, 166, 90–107.
110. Wang, D., Hu, M., Li, X., Zhang, D., Chen, C., Fu, J., *et al.* Design, synthesis, and evaluation of isoflavone analogs as multifunctional agents for the treatment of Alzheimer's disease. *Eur. J. Med. Chem*. **2019**, 168, 207–220.
111. Talele, T.T., Khedkar, S.A., Rigby, A.C. Successful applications of computer aided drug discovery: moving drugs from concept to the clinic. *Curr. Top. Med. Chem.* **2010**, 10(1), 127–141.
112. Bisht, N., Singh, B.K. Role of computer aided drug design in drug development and drug discovery. *IJPSR* **2018**, 9(4), 1405–1415.
113. (a) RCSB Protein Data Bank. Available online: https://rcsb.org (accessed online 29-May-2020); (b) Berman, H.M., Westbrook, J., Feng, Z., Gilliland, G., Bhat,

T.N., Weissig, H., Shindyalov, I.N., Bourne, P.E. The Protein Data Bank. *Nucleic Acids Res*. **2000**, 28, 235–242.
114. Sastry, G.M., Adzhigirey, M., Day, T., Annabhimoju, R., Sherman, W. Protein and ligand preparation: Parameters, protocols, and influence on virtual screening enrichments. *J. Comput. Aid. Mol. Des.* **2013**, 27, 221–234.
115. HyperChem 8.0 Molecular Modeling Package; Hypercube Software: Gainesville, FL.
116. Available online: https://cactus.nci.nih.gov/translate/ (accessed online 29-May-2020).
117. Schrödinger Release 2018–1: LigPrep, Schrödinger, LLC, New York, NY, **2018**.
118. Morris, G.M., Huey, R., Lindstrom, W., Sanner, M.F., Belew, R.K., Goodsell, D.S., *et al*. Autodock4 and AutoDockTools4: automated docking with selective receptor flexibility. *J. Comput. Chem.* **2009**, 16, 2785–2791.
119. Goodman, K.M., Kjaer, S., Beuron, F., Knowles, P.P., Nawrotek, A., Burns, E.M., *et al*. RET recognition of GDNF-GFRα1 ligand by a composite binding site promotes membrane-proximal self-association. *Cell Rep.* **2014**, 8(6), 1894–1904.
120. Parkash, V., Goldman, A. Comparison of GFL-GFRalpha complexes: further evidence relating GFL bend angle to RET signalling. *Acta. Crystallogr. Sect. F. Struct. Biol. Cryst. Commun.* **2009**, 65(Pt 6), 551–558.
121. Henderson, J.L., Kormos, B.L., Hayward, M.M., Coffman, K.J., Jasti, J., Kurumbail, R.G., *et al*. Discovery and preclinical profiling of 3-[4-(morpholin-4-yl)-7H-pyrrolo[2,3-d]pyrimidin-5-yl]benzonitrile (PF-06447475), a highly potent, selective, brain penetrant, and in vivo active LRRK2 kinase inhibitor. *J. Med. Chem.* **2015**, 58, 419–432.
122. Villemure, E., Volgraf, M., Jiang, Y., Wu, G., Ly, C.Q., Yuen, P.W., *et al*. GluN2A-Selective Pyridopyrimidinone Series of NMDAR Positive Allosteric Modulators with an Improved in Vivo Profile. *ACS Med. Chem. Lett.* **2017**, 8, 84–89.
123. Wang, T., Lamb, M.L., Block, M.H., Davies, A.M., Han, Y., Hoffmann, E., *et al*. Discovery of disubstituted imidazo[4,5-B]pyridines and purines as potent Trka inhibitors. *ACS Med. Chem. Lett.* **2012**, 3, 705.
124. Cheung, J., Rudolph, M.J., Burshteyn, F., Cassidy, M.S., Gary, E.N., Love, J., *et al*. Structures of human acetylcholinesterase in complex with pharmacologically important ligands. *J. Med. Chem.* **2012**, 55, 10282–10286.
125. Neumann, U., Ufer, M., Jacobson, L.H., Rouzade-Dominguez, M.L., Huledal, G., Kolly, C., *et al*. The BACE-1 inhibitor CNP520 for prevention trials in Alzheimer's disease. *EMBO Mol. Med.* **2018**, 10:e9316.
126. Bertrand, J.A., Thieffine, S., Vulpetti, A., Cristiani, C., Valsasina, B., Knapp, S., *et al.* Structural characterization of the GSK-3beta active site using selective and non-selective ATP-mimetic inhibitors. *J. Mol. Biol*. **2003**, 333, 393–407.
127. Coleman, J.A., Green, E.M., Gouaux, E. X-ray structures and mechanism of the human serotonin transporter. *Nature* **2016**, 532, 334–339.
128. Pagadala, N.S., Syed. K., Tuszynski, J. Software for molecular docking: a review. *Biophys. Rev.* **2017**, 9, 91–102.
129. Rarey, M., Kramer, B., Lengauer, T., Klebe, G. A fast-flexible docking method using an incremental construction algorithm. *J. Mol. Biol.* **1996**, 261(3), 470–489.
130. Kramer, B., Rarey, M., Lengauer, T. Evaluation of the FLEXX incremental construction algorithm for protein-ligand docking. *Proteins* **1999**, 37(2), 228–241.

131. Morris, G.M., Goodsell, D.S., Halliday, R.S., Huey, R., Hart, W.E., Belew, R.K., *et al*. Automated docking using a Lamarckian genetic algorithm and an empirical binding free energy function. *J. Comput. Chem.* **1998**, 19(14), 1639–1662.
132. Jones, G., Willett, P., Glen, R.C., Leach, A.R., Taylor, R. Development and validation of a genetic algorithm for flexible docking. *J. Mol. Biol.* **1997**, 267(3), 727–748.
133. Liu, M., Wang, S. MCDOCK: a Monte Carlo simulation approach to the molecular docking problem. *J. Comput. Aided Mol. Des.* **1999**, 13(5), 435–451.
134. Morris, G.M., Lim-Wilby, M. Molecular docking. *Methods Mol. Biol.* **2008**, 443, 365–382.
135. Huang, N., Shoichet, B.K., Irwin, J.J. Benchmarking sets for molecular docking. *J. Med. Chem.* **2006**, 49(23), 6789–6801.
136. Trott, O., Olson, A.J. AutoDock Vina: improving the speed and accuracy of docking with a new scoring function, efficient optimization and multithreading. *J. Comput. Chem.* **2010**, 31, 455–461.
137. Baxter, J. Local optima avoidance in depot location. *J. Oper. Res. Soc.* **1981**, 32(9), 815–819.
138. Blum, A.R.C., Blesa, M., Sampels, M. Hybrid Metaheuristics: an emerging approach to optimization. Springer-Verlag, **2008**.
139. Nocedal, J., Wright, S.J. Numerical optimization. Berlin: Springer Series in Operations Research, Springer Verlag, **1999**.
140. Jaghoori, M.M., Bleijlevens, B., Olabarriaga, S.D. 1001 Ways to run AutoDock Vina for virtual screening. *J. Comput. Aided Mol. Des.* **2016**, 30(3), 237–249.
141. Shityakov, S., Förster, C. In silico predictive model to determine vector-mediated transport properties for the blood-brain barrier choline transporter. *Adv. Appl. Bioinform. Chem.* **2014**, 7, 23–36.
142. Friesner, R.A., Banks, J.L., Murphy, R.B., Halgren, T.A., Klicic, J.J., Mainz, D.T., *et al*. Glide: a new approach for rapid, accurate docking and scoring. 1. Method and assessment of docking accuracy. *J. Med. Chem.* **2004**, 47, 1739–1749.
143. Friesner, R.A., Murphy, R.B., Repasky, M.P., Frye, L.L., Greenwood, J.R., Halgren, T.A., *et al*. Extra precision glide: docking and scoring incorporating a model of hydrophobic enclosure for protein-ligand complexes. *J. Med. Chem.* **2006**, 49, 6177–6196.
144. Halgren, T.A., Murphy, R.B., Friesner, R.A., Beard, H.S., Frye, L.L., Pollard, W.T., *et al*. Glide: a new approach for rapid, accurate docking and scoring. 2. Enrichment factors in database screening. *J. Med. Chem.* **2004**, 47, 1750–1759.
145. Rizzo, R.C., Jorgensen, W.L. OPLS all-atom model for amines: Resolution of the amine hydration problem. *J. Am. Chem. Soc.* **1999**, 121, 4827−4836.
146. Damm, W., Frontera, A., Tirado-Rives, J., Jorgensen, W.L. OPLS all-atom force field for carbohydrates. *J. Comput. Chem.* **1997**, 18, 1955−1970.
147. Jorgensen, W.L., Maxwell, D.S., Tirado-Rives, J. Development and testing of the OPLS all-atom force field on conformational energetics and properties of organic liquids. *J. Am. Chem. Soc.* **1996**, 118, 11225−11236.
148. Kaminski, G.A., Friesner, R.A., Tirado-Rives, J., Jorgensen, W.L. Evaluation and reparametrization of the OPLS-aa force field for proteins via comparison with accurate quantum chemical calculations on peptides. *J. Phys. Chem. B*. **2001**, 105, 6474−6487.
149. Jensen, K.P., Jorgensen, W.L. Halide, ammonium, and alkali metal ion parameters for modeling aqueous solutions. *J. Chem. Theory Comput.* **2006**, 2, 1499−1509.

150. Lennard-Jones, J.E. On the determination of molecular fields. *Proc. R. Soc. A* **1924**, 106(738), 463–477.
151. Schrödinger Release 2018–1: Glide, Schrödinger, LLC, New York, NY, *2018*.
152. Bowers, K.J., Chow, D.E., Xu, H., Dror, R.O., Eastwood, M.P., Gregersen, B.A., *et al*. Scalable algorithms for molecular dynamics simulations on commodity clusters. In: Proceedings of the ACM/IEEE SC 2006 conference, 43–43 (2006).
153. Zielkiewicz, J. Structural Properties of Water: Comparison of the SPC, SPCE, TIP4P, and TIP5P models of water. *J. Chem. Phys.* **2005**, 123, 104501; *J. Chem. Phys.* **2006**, 124, 109901.
154. Banks, J.L., Beard, H.S., Cao, Y., Cho, A.E., Damm, W., Farid, R., *et al*. Integrated Modeling Program, Applied Chemical Theory (IMPACT). *J. Comput. Chem.* **2005**, 26, 1752−1780.
155. Darden, T., York, D., Pedersen, L. Particle mesh Ewald: An N·log(N) method for Ewald sums in large systems. *J. Chem. Phys.* **1993**, 98, 10089.
156. Martyna, G.J., Klein, M.L. Nosé–Hoover Chains: the canonical ensemble via continuous dynamics. *J. Chem. Phys.* **1992**, 97, 2635–2643.
157. Christ, C.D., Mark, A.E., van Gunsteren, W.F. Basic ingredients of free energy calculations: A review. *J. Comput. Chem.* **2009**, 31, 1569−1582.
158. Li, A.J., Daggett, V. Characterization of the transition-state of protein unfolding by use of molecular dynamics – chymotrypsin inhibitor-2. *PNAS U. S. A.* **1994**, 91, 10430−10434.
159. Shaw, D.E., Maragakis, P., Lindorff-Larsen, K., Piana, S., Dror, R.O., Eastwood, M.P., *et al*. Atomic-level characterization of the structural dynamics of proteins. *Science* **2010**, 330, 341−346.
160. Hospital, A., Goni, J.R., Orozco, M., Gelpi, J.L. Molecular dynamics simulations: advances and applications. *Adv. Appl. Bioinform. Chem.* **2015**, 8, 37−47.
161. Genheden, S., Ryde, U. Comparison of end-point continuum solvation methods for the calculation of protein−ligand binding free energies. *Proteins: Struct. Funct. Genet.* **2012**, 80, 1326−1342.
162. Aqvist, J., Medina, C., Samuelsson, J.E. A New method for predicting binding affinity in computer aided drug design. *Protein Eng. Des. Sel.* **1994**, 7, 385−391.
163. Swanson, J.M., Henchman, R.H., McCammon, J.A. Revisiting free energy calculations: a theoretical connection to MM/PBSA and direct calculation of the association free energy. *Biophys. J.* **2004**, 86, 67−74.
164. Srinivasan, J., Cheatham, T.E., Cieplak, P., Kollman, P.A., Case, D.A. Continuum solvent studies of the stability of DNA, RNA, and phosphoramidate−DNA helices. *J. Am. Chem. Soc.* **1998**, 120, 9401−9409.
165. Srinivasan, J., Miller, J., Kollman, P.A., Case, D.A. Continuum solvent studies of the stability of RNA hairpin loops and helices. *J. Biomol. Struct. Dyn.* **1998**, 16, 671.
166. Kollman, P.A., Massova, I., Reyes, C., Kuhn, B., Huo, S., Chong, L., *et al*. Calculating structures and free energies of complex molecules: combining molecular mechanics and continuum models. *Acc. Chem. Res.* **2000**, 33, 889−897.
167. Zoete, V., Irving, M.B., Michielin, O. MM-GBSA binding free energy decomposition and T cell receptor engineering. *J. Mol. Recognit.* **2010**, 23, 142−152.
168. Zoete, V., Michielin, O. Comparison between computational alanine scanning and per-residue binding free energy decomposition for protein−protein association using MM-GBSA: application to the TCR-P MHC complex. *Proteins: Struct. Funct. Genet.* **2007**, 67, 1026−1047.

169. Gohlke, H., Kiel, C., Case, D.A. Insights into protein−protein binding by binding free energy calculation and free energy decomposition for the Ras-Raf and Ras-RalGDS complexes. *J. Mol. Biol.* **2003**, 330, 891−913.
170. Mongan, J., Simmerling, C., McCammon, J.A., Case, D.A., Onufriev, A. Generalized Born model with a simple, robust molecular volume correction. *J. Chem. Theory Comput*. **2007**, 3(1), 156–169.
171. www.graphpad.com, La Jolla California, USA (accessed online 29-May-2020).
172. Leppänen, V.-M., Bespalov, M.M., Runeberg-Roos, P., Puurand, Ü., Merits, A., Saarma, M., *et al*. The structure of GFRα1 domain 3 reveals new insights into GDNF binding and RET activation. *EMBO J.* **2004**, 23, 1452−1462.
173. Parkash, V., Leppänen, V.M., Virtanen, H., Jurvansuu, J.M., Bespalov, M.M., Sidorova, Y.A., *et al*. The structure of the glial cell line-derived neurotrophic factor-coreceptor complex: insights into RET signaling and heparin binding. *J. Biol. Chem.* **2008**, 283, 35164−35172.
174. Sterling, T., Irwin, J.J. ZINC 15 – Ligand Discovery for Everyone. *J. Chem. Inf. Model.* 55(11), 2324–2337.
175. http://www.molport.com/shop/index; MolPort: Lacplesa iela 41, Riga, LV-1011, Latvia (accessed online 29-May-2020).
176. Sidorova, Y.A., Matlik, K., Paveliev, M., Lindahl, M., Piranen, E., Milbrandt, J., *et al*. Persephin signaling through GFRα1: The potential for the treatment of Parkinson's disease. *Mol. Cell. Neurosci.* **2010**, 44, 223−232.
177. Meng, X.Y., Zhang, H.X., Mezei, M., Cui, M. Molecular docking: a powerful approach for structure-based drug discovery. *Curr. Comput. Aided Drug. Des.* **2011**, 7(2), 146–157.
178. Ambure, P., Bhat, J., Puzyn, T., Roy, K. Identifying natural compounds as multi-target-directed ligands against Alzheimer's disease: an in silico approach. *J. Biomol. Struct. Dyn.* **2018**, 23, 1.
179. Dos Santos, T.C., Gomes, T.M., Pinto, B.A.S., Camara, A.L., Paes, A.M.A. Naturally occurring acetylcholinesterase inhibitors and their potential use for Alzheimer's disease therapy. *Front. Pharmacol.* **2018**, 9, 1192.
180. Llorens-Martín, M., Jurado, J., Hernández, F., Avila, J. GSK-3β, a pivotal kinase in Alzheimer disease. *Front. Mol. Neurosci*. **2014**, 7, 46.
181. Coimbra, J.R.M., Marques, D.F.F., Baptista, S.J., Pereira, C.M.F., Moreira, P.I., Dinis, T.C.P., *et al*. Highlights in BACE1 inhibitors for Alzheimer's disease treatment. *Front. Chem.* **2018**, 6, 178.
182. Rodríguez, J.J., Noristani, H.N., Verkhratsky, A. The serotonergic system in ageing and Alzheimer's disease. *Progr. Neurobiol*. **2012**, 99, 15–41.
183. Bae, J.R., Lee, B.D. Function and dysfunction of leucine-rich repeat kinase 2 (LRRK2): Parkinson's disease and beyond. *BMB Rep*. **2015**, 48, 243–248.
184. Zhang, Y., Li, P., Feng, J., Wu, M. Dysfunction of NMDA receptors in Alzheimer's disease. *Neurol. Sci.* **2016**, 37, 1039–1047.
185. Zhou, O., Sheng, M. NMDA receptors in nervous system diseases. *Neuropharmacology* **2014**, 74, 69–75.
186. Moises, T., Wüller, S., Saxena, S., Senderek, J., Weis, J., Krüttgen, A. Proteasomal inhibition alters the trafficking of the neurotrophin receptor TrkA. *Biochem. Biophys. Res. Commun*. **2009**, 387, 360–364.
187. Hirose, M., Kuroda, Y., Murata, E. NGF/TrkA Signaling as a therapeutic target for pain. *Pain Pract*. **2016**, 16, 175.

188. Villemure, E., Volgraf, M., Jiang, Y., Wu, G., Ly, C.Q., Yuen, P.W., *et al*. GluN2A-selective pyridopyrimidinone series of NMDAR positive allosteric modulators with an improved in vivo profile. *ACS Med. Chem. Lett.* **2016**, 8(1), 84–89.
189. Daher, J.P., Abdelmotilib, H.A., Hu, X., Volpicelli-Daley, L.A., Moehle, M.S., Fraser, K.B., *et al*. Leucine-rich Repeat Kinase 2 (LRRK2) pharmacological inhibition abates α-synuclein gene-induced neurodegeneration. *J. Biol. Chem.* **2015**, 290(32), 19433–19444.
190. Thress, K., Macintyre, T., Wang, H., Whitston, D., Liu, Z.Y., Hoffmann, E., *et al*. Identification and preclinical characterization of AZ-23, a novel, selective, and orally bioavailable inhibitor of the Trk kinase pathway. *Mol. Cancer Ther.* **2009**, 8(7), 1818–1827.
191. Genheden, S., Ryde, U. The MM/PBSA and MM/GBSA methods to estimate ligand-binding affinities. *Expert Opin. Drug Discovery* **2015**, 10, 449−461.
192. Congreve, M., Carr, R., Murray, C., Jhoti, H. A 'rule of three' for fragment-based lead discovery? *Drug Discov. Today* **2003**, 8(19), 876–877.
193. Mao, F., Wang, H., Ni, W., Zheng, X., Wang, M., Bao, K., *et al*. Design, synthesis, and biological evaluation of orally available first-generation dual-target selective inhibitors of Acetylcholinesterase (AChE) and Phosphodiesterase 5 (PDE5) for the treatment of Alzheimer's disease. *ACS Chem. NeuroSci*. **2018**, 9, 328–345.
194. Gálvez, J., Polo, S., Insuasty, B., Gutiérrez, M., Cáceres, D., Alzate-Morales, J.H., *et al*. Design, facile synthesis, and evaluation of novel spiro- and pyrazolo[1,5-c]quinazolines as cholinesterase inhibitors: Molecular docking and MM/GBSA studies. *Comput. Biol. Chem.* **2018**, 74, 218–229.
195. Neumann, U., Ufer, M., Jacobson, L.H., Rouzade-Dominguez, M.L., Huledal, G., Kolly, C., *et al*. The BACE-1 inhibitor CNP520 for prevention trials in Alzheimer's disease. *EMBO Mol. Med.* **2018**, 10.
196. Rueeger, H., Lueoend, R., Rogel, O., Rondeau, J.-M., Möbitz, H., Machauer, R., *et al*. Discovery of cyclic sulfone hydroxyethylamines as potent and selective β-site APP-cleaving enzyme 1 (BACE1) inhibitors: Structure-based design and in vivo reduction of amyloid β-peptides. *J. Med. Chem.* **2012**, 55, 3364–3386.
197. Zou, Y., Li, L., Chen, W., Chen, T., Ma, L., Wang, X., *et al*. Virtual screening and structure-based discovery of indole acylguanidines as potent β-secretase (BACE1) inhibitors. *Molecules* **2013**, 18(5), 5706–5722.
198. Wagner, F.F., Benajiba, L., Campbell, A.J., Weïwer, M., Sacher, J.R., Gale, J.P., *et al*. Exploiting an Asp-Glu "switch" in glycogen synthase kinase 3 to design paralog-selective inhibitors for use in acute myeloid leukemia. *Sci. Transl. Med*. **2018**, 10(431), eaam8460.
199. Liang, S.H., Chen, J.M., Normandin, M.D., Chang, J.S., Chang, G.C., Taylor, C.K., *et al*. Discovery of a highly selective Glycogen Synthase Kinase-3 inhibitor (PF-04802367) that modulates Tau phosphorylation in the brain: translation for PET neuroimaging. *Angew. Chem. Int. Ed. Engl.* **2016**, 55, 9601–9605.
200. Sivaprakasam, P., Han, X., Civiello, R.L., Jacutin-Porte, S., Kish, K., Pokross, M., *et al*. Discovery of new acylaminopyridines as GSK-3 inhibitors by a structure guided in-depth exploration of chemical space around a pyrrolopyridinone core. *Bioorg. Med. Chem. Lett.* **2015**, 25(9), 1856–1863.
201. Davis, B.A., Nagarajan, A., Forrest, L.R., Singh, S.K. Mechanism of Paroxetine (Paxil) inhibition of the serotonin transporter. *Sci. Rep.* **2016**, 6, 23789.

202. Larsen, M.A.B., Plenge, P., Andersen, J., Eildal, J.N.N., Kristensen, A.S., Bøgesø, K.P., *et al*. Structure-activity relationship studies of citalopram derivatives: examining substituents conferring selectivity for the allosteric site in the serotonin transporter. *Br. J. Pharmacol*. **2016**, 173(5), 925–936.
203. Krout, D., Rodriquez, M., Brose, S.A., Golovko, M.Y., Henry, L.K., Thompson, B.J. Inhibition of the serotonin transporter is altered by metabolites of selective serotonin and norepinephrine reuptake inhibitors and represents a caution to acute or chronic treatment paradigms. *ACS Chem. Neurosci.* **2017**, 8(5), 1011–1018.

SUMMARY IN ESTONIAN

Aktiivsete ühendite disain neurodegeneratiivsete haiguste raviks

Erinevalt enamikust keharakkudest suur osa inimese närvirakke ei uuene. Vananemine, vigastused ja neurodegeneratiivsed haigused põhjustavad närvirakkude kängumist ja surma. Levinumate neurodegeneratiivsete haiguste hulka kuuluvad Parkinsoni tõbi, Alzheimeri tõbi, amüotroofne lateraalskleroos, Huntingtoni tõbi ja dementsus. Maailma Terviseorganisatsiooni (WHO) aruande kohaselt oli 2015. aastal dementsusehaigete koguarv maailmas 47 miljonit inimest, 2030. aastaks võib see kasvada 75 miljonini ja 2050. aastaks 132 miljonini. Samuti on WHO andmetel Alzheimeri tõbi ja teised dementsuse vormid maailmas kümne peamise surmapõhjuse hulgas. Väga suureks probleemiks on nende haiguste õigeaegne diagnoosimine haiguse algfaasis. Praegused raviks kasutatavad ravimid ja ravimeetodid ainult leevendavad haigustunnuseid, kuid ei suuda kõrvaldada haiguse põhjust ega pidurdada või peatada haiguse kulgu. Seega pakuvad väga suurt huvi otsingud uute ravimite leidmiseks.

Arvutitehnoloogia areng viimastel aastakümnetel on aidanud oluliselt kiirendada uute ravimite väljatöötamise pikka protsessi ja vähendada selle kulusid. Käesolevas doktoritöös rakendati tänapäevaseid molekulaarse modelleerimise meetodeid uute aktiivsete ühendite väljatöötamiseks neurodegeneratiivsete haigustega seotud bioloogiliste märklaudade, erinevate ensüümide ja retseptorvalkude vastu.

Töö esimeses osas viidi läbi gliia närvikasvfaktori GDNF perekonna retseptori GFRα1 ja selle varem leitud agonistide BT13 ja BT18 omavahelise toime ja seondumise mehhanismide detailne uuring ning otsingud leidmaks GDNFi toimet matkivaid keemilisi ühendeid ehk mimeetikuid. GDNF seondub spetsiifiliselt retseptorile GFRα1 ja see kompleks omakorda seondub transmembraanse türosiini kinaasi retseptorile RET, aktiveerides rakusisesed signaalirajad. **Artiklis I** leiti, et allosteeriline sait GFRα1 valgus on eelistatud ühendite BT13 ja BT18 seondumisel GDNF-GFRα1-RET kompleksiga. Arvestades, et uuritud ühendid on eksperimentaalselt kirjeldatud ka kui otsesed RET agonistid, võib siiski eeldada, et RET seondumiskoht GFRα1-ga muutub eelistatavaks membraani seotud RET-olekus. See võimaldaks neil ühenditel toimida otseste RET agonistidena. **Artiklis II** kasutati struktuuri-põhist ravimidisaini, leidmaks uut potentsiaalset GDNFi perekonna retseptori GFRα1 agonisti, millel on erinev RET aktiveerimise mehhanism. Kuigi leitud ühend on bioloogiliselt väheaktiivne, on see siiski esimene ühend, mis aktiveerib otseselt GDNFi retseptorit RET retseptori GFRα1 kaudu endogeense närvikasvufaktori puudumisel, mis muudab selle selektiivsemaks kui varem kirjeldatud ühendid BT13 ja BT18.

Töö teises osas rakendati struktuur-omadus sõltuvustel (QSAR) põhinevate ja molekulaarse modelleerimise meetodite kombinatsiooni uute ravimikandidaatide väljatöötamisel neurodegeneratiivsete haiguste vastu. **Artiklis III** uuriti

in silico looduslikke ühendeid, mille tulemusena tuvastati vastavalt Alzheimeri tõve, Parkinsoni tõve ja neuropaatilise valuga seotud sihtmärkide NMDA, LRRK2 ja TrkA jaoks mitmed uued potentsiaalsete inhibiitorite kandidaadid. **Artiklis IV** otsiti ravimikandidaate, lähtudes erinevatest Alzheimeri tõvega seotud valgu sihtmärkidest AChE, SERT, BACE1 ja GSK3β. Tuvastati ühend, mis toimib mikromolaarse inhibeeriva aktiivsusega kahe sihtmärgi (AChE ja BACE1) vastu. Leitud ühendite molekulaarse struktuuri edasine optimeerimine võimaldab leida uusi efektiivseid ravimikandidaate uuritud sihtvalkude vastu.

Kokkuvõtvalt, käesoleva doktoritöö käigus uuriti kaheksat neurodegeneratiivsete haigustega seotud valgu sihtmärki. Saadud andmed ja leitud uued aktiivsed ühendid võivad olla aluseks neurodegeneratiivsete haiguste raviks mõeldud ravimite edasisel väljatöötamisel, samuti nende haiguste arengu ja tekkemehhanismide sügavamal mõistmisel.

ACKNOWLEDGEMENTS

First of all, I would like to sincerely thank my supervisor Prof. Mati Karelson with great respect for his guidance, motivation, and support that he has provided throughout my study. It was a great honour for me to work under his guidance! I would like to thank my co-supervisor Dr. Jaana Tammiku-Taul for her guidance, useful advice, constructive feedback, and support during all the years of my work. I am very grateful to all my colleagues for their support and excellent working atmosphere. My deepest thanks to my co-authors for their invaluable contribution to our publications.

I am very thankful to my family and friends for their love, understanding, and motivation during these years. Special thanks to my husband and son for their infinite optimism and faith in me.

PUBLICATIONS

CURRICULUM VITAE

Name	Larisa Ivanova
Date of birth	December 26th, 1987
Citizenship	Russian
Address	Institute of Chemistry, University of Tartu, Ravila 14A, 50411, Tartu, Estonia
E-mail	larisa.ivanova@ut.ee

Education

2015–…	University of Tartu, Molecular Engineering, PhD student
2010–2012	Postgraduate student, Organic Chemistry, D.N. Pryanishnikov Perm State Agro-Technological University, Perm, Russia
2005–2010	Diploma of Specialist in Organic Chemistry, Perm State University, Perm, Russia

Professional employment

2016–…	University of Tartu, Institute of Chemistry, Chemist (1.0)
2011–2012	"TD Fregat" Ltd., Manufacturing Engineer (1.0)
2010–2011	"Snabinvest" Ltd., Manufacturing Engineer (1.0)

Professional self-improvement

2019	Structure-based drug design using the Schrödinger suite workshop, April 10, 2019, Moscow, Russia.

Scientific publications

Ivanova, L.; Tammiku-Taul, J.; Sidorova, Y.; Saarma, M.; Karelson, M. Small-Molecule Ligands as Potential GDNF Family Receptor Agonists. *ACS Omega* **2018**, *3(1)*, 1022–1030.

Ivanova, L.; Tammiku-Taul, J.; García-Sosa, A.T.; Sidorova, Y.; Saarma, M.; Karelson, M. Molecular Dynamics Simulations of the Interactions between Glial Cell Line-Derived Neurotrophic Factor Family Receptor GFRα1 and Small-Molecule Ligands. *ACS Omega* **2018**, *3(9)*, 11407–11414.

Ivanova, L.; Karelson, M.; Dobchev, D.A. Identification of Natural Compounds against Neurodegenerative Diseases Using in Silico Techniques. *Molecules* **2018**, *23(8)*, 1847.

Ivanova, L.; Karelson, M.; Dobchev, D.A. Multitarget Approach to Drug Candidates against Alzheimer's Disease Related to AChE, SERT, BACE1 and GSK3β Protein Targets. *Molecules* **2020**, *25(8)*, 1846.

Oral presentation

Ivanova, L.; Rausalu, K.; Žusinaite, E.; Karelson, M.; Merits, A. Ligand-based approach to *in silico* design of a potential Chikungunya virus protease inhibitor. XXV Symposium "Bioinformatics and Computer Aided Drug Discovery", April 08–09, 2019, Moscow, Russia.

Poster presentations

Ivanova, L.; Tammiku-Taul, J.; Karelson, M. Molecular dynamics simulations of the glial cell line-derived neurotrophic factor (GDNF) family receptor GFRα1–ligand interactions. 22nd European Symposium on Quantitative Structure-Activity Relationships (EuroQSAR), September 16–20, 2018, Thessaloniki, Greece.

Ivanova, L.; Rausalu, K.; Žusinaite, E.; Merits, A.; Karelson, M. Ligand-based approach to *in silico* design of a potential Chikungunya virus protease inhibitor. 22nd European Symposium on Quantitative Structure-Activity Relationships (EuroQSAR), September 16–20, 2018, Thessaloniki, Greece.

ELULOOKIRJELDUS

Nimi Larisa Ivanova
Sünniaeg 26. detsember, 1987
Kodakondsus Venemaa
Aadress Keemia instituut, Tartu Ülikool, Ravila 14A, 50411, Tartu, Eesti
E-mail larisa.ivanova@ut.ee

Haridus

2015–…	Tartu Ülikool, doktoriõpe, molekulaartehnoloogia
2010–2012	D. Prjanišnikovi nimeline Riiklik Põllumajandusakadeemia, aspirant, orgaaniline keemia
2005–2010	Permi Riiklik Ülikool, spetsialist (integreeritud õpe), orgaaniline keemia

Teenistuskäik

2016–…	Tartu Ülikool, Keemia instituut, keemik (1,0)
2011–2012	OÜ „TD Fregat“, insener-tehnoloog (1,0)
2010–2011	OÜ „Snabinvest“, insener-tehnoloog (1,0)

Erialane enesetäiendus

2019	*Structure-based drug design using the Schrödinger suite workshop*, 10. aprill 2019, Moskva, Venemaa.

Teaduspublikatsioonid

Ivanova, L.; Tammiku-Taul, J.; Sidorova, Y.; Saarma, M.; Karelson, M. Small-Molecule Ligands as Potential GDNF Family Receptor Agonists. *ACS Omega* **2018**, *3(1)*, 1022–1030.

Ivanova, L.; Tammiku-Taul, J.; García-Sosa, A.T.; Sidorova, Y.; Saarma, M.; Karelson, M. Molecular Dynamics Simulations of the Interactions between Glial Cell Line-Derived Neurotrophic Factor Family Receptor GFRα1 and Small-Molecule Ligands. *ACS Omega* **2018**, *3(9)*, 11407–11414.

Ivanova, L.; Karelson, M.; Dobchev, D.A. Identification of Natural Compounds against Neurodegenerative Diseases Using In Silico Techniques. *Molecules* **2018**, *23(8)*, 1847.

Ivanova, L.; Karelson, M.; Dobchev, D.A. Multitarget Approach to Drug Candidates against Alzheimer's Disease Related to AChE, SERT, BACE1 and GSK3β Protein Targets. *Molecules* **2020**, *25(8)*, 1846.

Suuline ettekanne

Ivanova, L.; Rausalu, K.; Žusinaite, E.; Karelson, M.; Merits, A. Ligand-based approach to *in silico* design of a potential Chikungunya virus protease inhibitor. *XXV Symposium "Bioinformatics and Computer Aided Drug Discovery"*, 8.–9. aprill 2019, Moskva, Venemaa.

Posterettekanded

Ivanova, L.; Tammiku-Taul, J.; Karelson, M. Molecular dynamics simulations of the glial cell line-derived neurotrophic factor (GDNF) family receptor GFRα1–ligand interactions. *22nd European Symposium on Quantitative Structure-Activity Relationships (EuroQSAR)*, 16.–20. september 2018, Thessaloniki, Kreeka.

Ivanova, L.; Rausalu, K.; Žusinaite, E.; Merits, A.; Karelson, M. Ligand-based approach to *in silico* design of a potential Chikungunya virus protease inhibitor. *22nd European Symposium on Quantitative Structure-Activity Relationships (EuroQSAR)*, 16.–20. september 2018, Thessaloniki, Kreeka.

DISSERTATIONES CHIMICAE UNIVERSITATIS TARTUENSIS

1. **Toomas Tamm.** Quantum-chemical simulation of solvent effects. Tartu, 1993, 110 p.
2. **Peeter Burk.** Theoretical study of gas-phase acid-base equilibria. Tartu, 1994, 96 p.
3. **Victor Lobanov.** Quantitative structure-property relationships in large descriptor spaces. Tartu, 1995, 135 p.
4. **Vahur Mäemets.** The ^{17}O and ^{1}H nuclear magnetic resonance study of H_2O in individual solvents and its charged clusters in aqueous solutions of electrolytes. Tartu, 1997, 140 p.
5. **Andrus Metsala.** Microcanonical rate constant in nonequilibrium distribution of vibrational energy and in restricted intramolecular vibrational energy redistribution on the basis of slater's theory of unimolecular reactions. Tartu, 1997, 150 p.
6. **Uko Maran.** Quantum-mechanical study of potential energy surfaces in different environments. Tartu, 1997, 137 p.
7. **Alar Jänes.** Adsorption of organic compounds on antimony, bismuth and cadmium electrodes. Tartu, 1998, 219 p.
8. **Kaido Tammeveski.** Oxygen electroreduction on thin platinum films and the electrochemical detection of superoxide anion. Tartu, 1998, 139 p.
9. **Ivo Leito.** Studies of Brønsted acid-base equilibria in water and non-aqueous media. Tartu, 1998, 101 p.
10. **Jaan Leis.** Conformational dynamics and equilibria in amides. Tartu, 1998, 131 p.
11. **Toonika Rinken.** The modelling of amperometric biosensors based on oxidoreductases. Tartu, 2000, 108 p.
12. **Dmitri Panov.** Partially solvated Grignard reagents. Tartu, 2000, 64 p.
13. **Kaja Orupõld.** Treatment and analysis of phenolic wastewater with microorganisms. Tartu, 2000, 123 p.
14. **Jüri Ivask.** Ion Chromatographic determination of major anions and cations in polar ice core. Tartu, 2000, 85 p.
15. **Lauri Vares.** Stereoselective Synthesis of Tetrahydrofuran and Tetrahydropyran Derivatives by Use of Asymmetric Horner-Wadsworth-Emmons and Ring Closure Reactions. Tartu, 2000, 184 p.
16. **Martin Lepiku.** Kinetic aspects of dopamine D_2 receptor interactions with specific ligands. Tartu, 2000, 81 p.
17. **Katrin Sak.** Some aspects of ligand specificity of P2Y receptors. Tartu, 2000, 106 p.
18. **Vello Pällin.** The role of solvation in the formation of iotsitch complexes. Tartu, 2001, 95 p.
19. **Katrin Kollist.** Interactions between polycyclic aromatic compounds and humic substances. Tartu, 2001, 93 p.

20. **Ivar Koppel.** Quantum chemical study of acidity of strong and superstrong Brønsted acids. Tartu, 2001, 104 p.
21. **Viljar Pihl.** The study of the substituent and solvent effects on the acidity of OH and CH acids. Tartu, 2001, 132 p.
22. **Natalia Palm.** Specification of the minimum, sufficient and significant set of descriptors for general description of solvent effects. Tartu, 2001, 134 p.
23. **Sulev Sild.** QSPR/QSAR approaches for complex molecular systems. Tartu, 2001, 134 p.
24. **Ruslan Petrukhin.** Industrial applications of the quantitative structure-property relationships. Tartu, 2001, 162 p.
25. **Boris V. Rogovoy.** Synthesis of (benzotriazolyl)carboximidamides and their application in relations with *N*- and *S*-nucleophyles. Tartu, 2002, 84 p.
26. **Koit Herodes.** Solvent effects on UV-vis absorption spectra of some solvatochromic substances in binary solvent mixtures: the preferential solvation model. Tartu, 2002, 102 p.
27. **Anti Perkson.** Synthesis and characterisation of nanostructured carbon. Tartu, 2002, 152 p.
28. **Ivari Kaljurand.** Self-consistent acidity scales of neutral and cationic Brønsted acids in acetonitrile and tetrahydrofuran. Tartu, 2003, 108 p.
29. **Karmen Lust.** Adsorption of anions on bismuth single crystal electrodes. Tartu, 2003, 128 p.
30. **Mare Piirsalu.** Substituent, temperature and solvent effects on the alkaline hydrolysis of substituted phenyl and alkyl esters of benzoic acid. Tartu, 2003, 156 p.
31. **Meeri Sassian.** Reactions of partially solvated Grignard reagents. Tartu, 2003, 78 p.
32. **Tarmo Tamm.** Quantum chemical modelling of polypyrrole. Tartu, 2003. 100 p.
33. **Erik Teinemaa.** The environmental fate of the particulate matter and organic pollutants from an oil shale power plant. Tartu, 2003. 102 p.
34. **Jaana Tammiku-Taul.** Quantum chemical study of the properties of Grignard reagents. Tartu, 2003. 120 p.
35. **Andre Lomaka.** Biomedical applications of predictive computational chemistry. Tartu, 2003. 132 p.
36. **Kostyantyn Kirichenko.** Benzotriazole – Mediated Carbon–Carbon Bond Formation. Tartu, 2003. 132 p.
37. **Gunnar Nurk.** Adsorption kinetics of some organic compounds on bismuth single crystal electrodes. Tartu, 2003, 170 p.
38. **Mati Arulepp.** Electrochemical characteristics of porous carbon materials and electrical double layer capacitors. Tartu, 2003, 196 p.
39. **Dan Cornel Fara.** QSPR modeling of complexation and distribution of organic compounds. Tartu, 2004, 126 p.
40. **Riina Mahlapuu.** Signalling of galanin and amyloid precursor protein through adenylate cyclase. Tartu, 2004, 124 p.

41. **Mihkel Kerikmäe.** Some luminescent materials for dosimetric applications and physical research. Tartu, 2004, 143 p.
42. **Jaanus Kruusma.** Determination of some important trace metal ions in human blood. Tartu, 2004, 115 p.
43. **Urmas Johanson.** Investigations of the electrochemical properties of polypyrrole modified electrodes. Tartu, 2004, 91 p.
44. **Kaido Sillar.** Computational study of the acid sites in zeolite ZSM-5. Tartu, 2004, 80 p.
45. **Aldo Oras.** Kinetic aspects of dATPαS interaction with $P2Y_1$ receptor. Tartu, 2004, 75 p.
46. **Erik Mölder.** Measurement of the oxygen mass transfer through the air-water interface. Tartu, 2005, 73 p.
47. **Thomas Thomberg.** The kinetics of electroreduction of peroxodisulfate anion on cadmium (0001) single crystal electrode. Tartu, 2005, 95 p.
48. **Olavi Loog.** Aspects of condensations of carbonyl compounds and their imine analogues. Tartu, 2005, 83 p.
49. **Siim Salmar.** Effect of ultrasound on ester hydrolysis in aqueous ethanol. Tartu, 2006, 73 p.
50. **Ain Uustare.** Modulation of signal transduction of heptahelical receptors by other receptors and G proteins. Tartu, 2006, 121 p.
51. **Sergei Yurchenko.** Determination of some carcinogenic contaminants in food. Tartu, 2006, 143 p.
52. **Kaido Tämm.** QSPR modeling of some properties of organic compounds. Tartu, 2006, 67 p.
53. **Olga Tšubrik.** New methods in the synthesis of multisubstituted hydrazines. Tartu. 2006, 183 p.
54. **Lilli Sooväli.** Spectrophotometric measurements and their uncertainty in chemical analysis and dissociation constant measurements. Tartu, 2006, 125 p.
55. **Eve Koort.** Uncertainty estimation of potentiometrically measured ph and pK_a values. Tartu, 2006, 139 p.
56. **Sergei Kopanchuk.** Regulation of ligand binding to melanocortin receptor subtypes. Tartu, 2006, 119 p.
57. **Silvar Kallip.** Surface structure of some bismuth and antimony single crystal electrodes. Tartu, 2006, 107 p.
58. **Kristjan Saal.** Surface silanization and its application in biomolecule coupling. Tartu, 2006, 77 p.
59. **Tanel Tätte.** High viscosity $Sn(OBu)_4$ oligomeric concentrates and their applications in technology. Tartu, 2006, 91 p.
60. **Dimitar Atanasov Dobchev**. Robust QSAR methods for the prediction of properties from molecular structure. Tartu, 2006, 118 p.
61. **Hannes Hagu**. Impact of ultrasound on hydrophobic interactions in solutions. Tartu, 2007, 81 p.
62. **Rutha Jäger.** Electroreduction of peroxodisulfate anion on bismuth electrodes. Tartu, 2007, 142 p.

63. **Kaido Viht.** Immobilizable bisubstrate-analogue inhibitors of basophilic protein kinases: development and application in biosensors. Tartu, 2007, 88 p.
64. **Eva-Ingrid Rõõm.** Acid-base equilibria in nonpolar media. Tartu, 2007, 156 p.
65. **Sven Tamp.** DFT study of the cesium cation containing complexes relevant to the cesium cation binding by the humic acids. Tartu, 2007, 102 p.
66. **Jaak Nerut.** Electroreduction of hexacyanoferrate(III) anion on Cadmium (0001) single crystal electrode. Tartu, 2007, 180 p.
67. **Lauri Jalukse.** Measurement uncertainty estimation in amperometric dissolved oxygen concentration measurement. Tartu, 2007, 112 p.
68. **Aime Lust.** Charge state of dopants and ordered clusters formation in CaF_2:Mn and CaF_2:Eu luminophors. Tartu, 2007, 100 p.
69. **Iiris Kahn**. Quantitative Structure-Activity Relationships of environmentally relevant properties. Tartu, 2007, 98 p.
70. **Mari Reinik.** Nitrates, nitrites, N-nitrosamines and polycyclic aromatic hydrocarbons in food: analytical methods, occurrence and dietary intake. Tartu, 2007, 172 p.
71. **Heili Kasuk.** Thermodynamic parameters and adsorption kinetics of organic compounds forming the compact adsorption layer at Bi single crystal electrodes. Tartu, 2007, 212 p.
72. **Erki Enkvist.** Synthesis of adenosine-peptide conjugates for biological applications. Tartu, 2007, 114 p.
73. **Svetoslav Hristov Slavov**. Biomedical applications of the QSAR approach. Tartu, 2007, 146 p.
74. **Eneli Härk.** Electroreduction of complex cations on electrochemically polished Bi(*hkl*) single crystal electrodes. Tartu, 2008, 158 p.
75. **Priit Möller.** Electrochemical characteristics of some cathodes for medium temperature solid oxide fuel cells, synthesized by solid state reaction technique. Tartu, 2008, 90 p.
76. **Signe Viggor.** Impact of biochemical parameters of genetically different pseudomonads at the degradation of phenolic compounds. Tartu, 2008, 122 p.
77. **Ave Sarapuu.** Electrochemical reduction of oxygen on quinone-modified carbon electrodes and on thin films of platinum and gold. Tartu, 2008, 134 p.
78. **Agnes Kütt.** Studies of acid-base equilibria in non-aqueous media. Tartu, 2008, 198 p.
79. **Rouvim Kadis.** Evaluation of measurement uncertainty in analytical chemistry: related concepts and some points of misinterpretation. Tartu, 2008, 118 p.
80. **Valter Reedo.** Elaboration of IVB group metal oxide structures and their possible applications. Tartu, 2008, 98 p.
81. **Aleksei Kuznetsov.** Allosteric effects in reactions catalyzed by the cAMP-dependent protein kinase catalytic subunit. Tartu, 2009, 133 p.

82. **Aleksei Bredihhin.** Use of mono- and polyanions in the synthesis of multisubstituted hydrazine derivatives. Tartu, 2009, 105 p.
83. **Anu Ploom.** Quantitative structure-reactivity analysis in organosilicon chemistry. Tartu, 2009, 99 p.
84. **Argo Vonk.** Determination of adenosine A_{2A}- and dopamine D_1 receptor-specific modulation of adenylate cyclase activity in rat striatum. Tartu, 2009, 129 p.
85. **Indrek Kivi.** Synthesis and electrochemical characterization of porous cathode materials for intermediate temperature solid oxide fuel cells. Tartu, 2009, 177 p.
86. **Jaanus Eskusson.** Synthesis and characterisation of diamond-like carbon thin films prepared by pulsed laser deposition method. Tartu, 2009, 117 p.
87. **Marko Lätt.** Carbide derived microporous carbon and electrical double layer capacitors. Tartu, 2009, 107 p.
88. **Vladimir Stepanov.** Slow conformational changes in dopamine transporter interaction with its ligands. Tartu, 2009, 103 p.
89. **Aleksander Trummal.** Computational Study of Structural and Solvent Effects on Acidities of Some Brønsted Acids. Tartu, 2009, 103 p.
90. **Eerold Vellemäe.** Applications of mischmetal in organic synthesis. Tartu, 2009, 93 p.
91. **Sven Parkel.** Ligand binding to 5-HT_{1A} receptors and its regulation by Mg^{2+} and Mn^{2+}. Tartu, 2010, 99 p.
92. **Signe Vahur.** Expanding the possibilities of ATR-FT-IR spectroscopy in determination of inorganic pigments. Tartu, 2010, 184 p.
93. **Tavo Romann**. Preparation and surface modification of bismuth thin film, porous, and microelectrodes. Tartu, 2010, 155 p.
94. **Nadežda Aleksejeva.** Electrocatalytic reduction of oxygen on carbon nanotube-based nanocomposite materials. Tartu, 2010, 147 p.
95. **Marko Kullapere.** Electrochemical properties of glassy carbon, nickel and gold electrodes modified with aryl groups. Tartu, 2010, 233 p.
96. **Liis Siinor.** Adsorption kinetics of ions at Bi single crystal planes from aqueous electrolyte solutions and room-temperature ionic liquids. Tartu, 2010, 101 p.
97. **Angela Vaasa.** Development of fluorescence-based kinetic and binding assays for characterization of protein kinases and their inhibitors. Tartu 2010, 101 p.
98. **Indrek Tulp.** Multivariate analysis of chemical and biological properties. Tartu 2010, 105 p.
99. **Aare Selberg.** Evaluation of environmental quality in Northern Estonia by the analysis of leachate. Tartu 2010, 117 p.
100. **Darja Lavõgina.** Development of protein kinase inhibitors based on adenosine analogue-oligoarginine conjugates. Tartu 2010, 248 p.
101. **Laura Herm.** Biochemistry of dopamine D_2 receptors and its association with motivated behaviour. Tartu 2010, 156 p.

102. **Terje Raudsepp.** Influence of dopant anions on the electrochemical properties of polypyrrole films. Tartu 2010, 112 p.
103. **Margus Marandi.** Electroformation of Polypyrrole Films: *In-situ* AFM and STM Study. Tartu 2011, 116 p.
104. **Kairi Kivirand.** Diamine oxidase-based biosensors: construction and working principles. Tartu, 2011, 140 p.
105. **Anneli Kruve.** Matrix effects in liquid-chromatography electrospray mass-spectrometry. Tartu, 2011, 156 p.
106. **Gary Urb.** Assessment of environmental impact of oil shale fly ash from PF and CFB combustion. Tartu, 2011, 108 p.
107. **Nikita Oskolkov.** A novel strategy for peptide-mediated cellular delivery and induction of endosomal escape. Tartu, 2011, 106 p.
108. **Dana Martin.** The QSPR/QSAR approach for the prediction of properties of fullerene derivatives. Tartu, 2011, 98 p.
109. **Säde Viirlaid.** Novel glutathione analogues and their antioxidant activity. Tartu, 2011, 106 p.
110. **Ülis Sõukand.** Simultaneous adsorption of Cd^{2+}, Ni^{2+}, and Pb^{2+} on peat. Tartu, 2011, 124 p.
111. **Lauri Lipping.** The acidity of strong and superstrong Brønsted acids, an outreach for the "limits of growth": a quantum chemical study. Tartu, 2011, 124 p.
112. **Heisi Kurig.** Electrical double-layer capacitors based on ionic liquids as electrolytes. Tartu, 2011, 146 p.
113. **Marje Kasari.** Bisubstrate luminescent probes, optical sensors and affinity adsorbents for measurement of active protein kinases in biological samples. Tartu, 2012, 126 p.
114. **Kalev Takkis.** Virtual screening of chemical databases for bioactive molecules. Tartu, 2012, 122 p.
115. **Ksenija Kisseljova**. Synthesis of aza-β^3-amino acid containing peptides and kinetic study of their phosphorylation by protein kinase A. Tartu, 2012, 104 p.
116. **Riin Rebane.** Advanced method development strategy for derivatization LC/ESI/MS. Tartu, 2012, 184 p.
117. **Vladislav Ivaništšev.** Double layer structure and adsorption kinetics of ions at metal electrodes in room temperature ionic liquids. Tartu, 2012, 128 p.
118. **Irja Helm.** High accuracy gravimetric Winkler method for determination of dissolved oxygen. Tartu, 2012, 139 p.
119. **Karin Kipper.** Fluoroalcohols as Components of LC-ESI-MS Eluents: Usage and Applications. Tartu, 2012, 164 p.
120. **Arno Ratas.** Energy storage and transfer in dosimetric luminescent materials. Tartu, 2012, 163 p.
121. **Reet Reinart-Okugbeni**. Assay systems for characterisation of subtype-selective binding and functional activity of ligands on dopamine receptors. Tartu, 2012, 159 p.

122. **Lauri Sikk.** Computational study of the Sonogashira cross-coupling reaction. Tartu, 2012, 81 p.
123. **Karita Raudkivi.** Neurochemical studies on inter-individual differences in affect-related behaviour of the laboratory rat. Tartu, 2012, 161 p.
124. **Indrek Saar.** Design of GalR2 subtype specific ligands: their role in depression-like behavior and feeding regulation. Tartu, 2013, 126 p.
125. **Ann Laheäär.** Electrochemical characterization of alkali metal salt based non-aqueous electrolytes for supercapacitors. Tartu, 2013, 127 p.
126. **Kerli Tõnurist.** Influence of electrospun separator materials properties on electrochemical performance of electrical double-layer capacitors. Tartu, 2013, 147 p.
127. **Kaija Põhako-Esko.** Novel organic and inorganic ionogels: preparation and characterization. Tartu, 2013, 124 p.
128. **Ivar Kruusenberg.** Electroreduction of oxygen on carbon nanomaterial-based catalysts. Tartu, 2013, 191 p.
129. **Sander Piiskop.** Kinetic effects of ultrasound in aqueous acetonitrile solutions. Tartu, 2013, 95 p.
130. **Ilona Faustova**. Regulatory role of L-type pyruvate kinase N-terminal domain. Tartu, 2013, 109 p.
131. **Kadi Tamm.** Synthesis and characterization of the micro-mesoporous anode materials and testing of the medium temperature solid oxide fuel cell single cells. Tartu, 2013, 138 p.
132. **Iva Bozhidarova Stoyanova-Slavova.** Validation of QSAR/QSPR for regulatory purposes. Tartu, 2013, 109 p.
133. **Vitali Grozovski**. Adsorption of organic molecules at single crystal electrodes studied by *in situ* STM method. Tartu, 2014, 146 p.
134. **Santa Veikšina**. Development of assay systems for characterisation of ligand binding properties to melanocortin 4 receptors. Tartu, 2014, 151 p.
135. **Jüri Liiv.** PVDF (polyvinylidene difluoride) as material for active element of twisting-ball displays. Tartu, 2014, 111 p.
136. **Kersti Vaarmets.** Electrochemical and physical characterization of pristine and activated molybdenum carbide-derived carbon electrodes for the oxygen electroreduction reaction. Tartu, 2014, 131 p.
137. **Lauri Tõntson**. Regulation of G-protein subtypes by receptors, guanine nucleotides and Mn^{2+}. Tartu, 2014, 105 p.
138. **Aiko Adamson.** Properties of amine-boranes and phosphorus analogues in the gas phase. Tartu, 2014, 78 p.
139. **Elo Kibena**. Electrochemical grafting of glassy carbon, gold, highly oriented pyrolytic graphite and chemical vapour deposition-grown graphene electrodes by diazonium reduction method. Tartu, 2014, 184 p.
140. **Teemu Näykki.** Novel Tools for Water Quality Monitoring – From Field to Laboratory. Tartu, 2014, 202 p.
141. **Karl Kaupmees.** Acidity and basicity in non-aqueous media: importance of solvent properties and purity. Tartu, 2014, 128 p.

142. **Oleg Lebedev**. Hydrazine polyanions: different strategies in the synthesis of heterocycles. Tartu, 2015, 118 p.
143. **Geven Piir.** Environmental risk assessment of chemicals using QSAR methods. Tartu, 2015, 123 p.
144. **Olga Mazina.** Development and application of the biosensor assay for measurements of cyclic adenosine monophosphate in studies of G protein-coupled receptor signalinga. Tartu, 2015, 116 p.
145. **Sandip Ashokrao Kadam.** Anion receptors: synthesis and accurate binding measurements. Tartu, 2015, 116 p.
146. **Indrek Tallo.** Synthesis and characterization of new micro-mesoporous carbide derived carbon materials for high energy and power density electrical double layer capacitors. Tartu, 2015, 148 p.
147. **Heiki Erikson.** Electrochemical reduction of oxygen on nanostructured palladium and gold catalysts. Tartu, 2015, 204 p.
148. **Erik Anderson.** *In situ* Scanning Tunnelling Microscopy studies of the interfacial structure between Bi(111) electrode and a room temperature ionic liquid. Tartu, 2015, 118 p.
149. **Girinath G. Pillai.** Computational Modelling of Diverse Chemical, Biochemical and Biomedical Properties. Tartu, 2015, 140 p.
150. **Piret Pikma.** Interfacial structure and adsorption of organic compounds at Cd(0001) and Sb(111) electrodes from ionic liquid and aqueous electrolytes: an *in situ* STM study. Tartu, 2015, 126 p.
151. **Ganesh babu Manoharan.** Combining chemical and genetic approaches for photoluminescence assays of protein kinases. Tartu, 2016, 126 p.
152. **Carolin Siimenson**. Electrochemical characterization of halide ion adsorption from liquid mixtures at Bi(111) and pyrolytic graphite electrode surface. Tartu, 2016, 110 p.
153. **Asko Laaniste.** Comparison and optimisation of novel mass spectrometry ionisation sources. Tartu, 2016, 156 p.
154. **Hanno Evard.** Estimating limit of detection for mass spectrometric analysis methods. Tartu, 2016, 224 p.
155. **Kadri Ligi.** Characterization and application of protein kinase-responsive organic probes with triplet-singlet energy transfer. Tartu, 2016, 122 p.
156. **Margarita Kagan.** Biosensing penicillins' residues in milk flows. Tartu, 2016, 130 p.
157. **Marie Kriisa.** Development of protein kinase-responsive photoluminescent probes and cellular regulators of protein phosphorylation. Tartu, 2016, 106 p.
158. **Mihkel Vestli.** Ultrasonic spray pyrolysis deposited electrolyte layers for intermediate temperature solid oxide fuel cells. Tartu, 2016, 156 p.
159. **Silver Sepp**. Influence of porosity of the carbide-derived carbon on the properties of the composite electrocatalysts and characteristics of polymer electrolyte fuel cells. Tartu, 2016, 137 p.
160. **Kristjan Haav**. Quantitative relative equilibrium constant measurements in supramolecular chemistry. Tartu, 2017, 158 p.

161. **Anu Teearu**. Development of MALDI-FT-ICR-MS methodology for the analysis of resinous materials. Tartu, 2017, 205 p.
162. **Taavi Ivan**. Bifunctional inhibitors and photoluminescent probes for studies on protein complexes. Tartu, 2017, 140 p.
163. **Maarja-Liisa Oldekop**. Characterization of amino acid derivatization reagents for LC-MS analysis. Tartu, 2017, 147 p.
164. **Kristel Jukk**. Electrochemical reduction of oxygen on platinum- and palladium-based nanocatalysts. Tartu, 2017, 250 p.
165. **Siim Kukk**. Kinetic aspects of interaction between dopamine transporter and *N*-substituted nortropane derivatives. Tartu, 2017, 107 p.
166. **Birgit Viira**. Design and modelling in early drug development in targeting HIV-1 reverse transcriptase and Malaria. Tartu, 2017, 172 p.
167. **Rait Kivi**. Allostery in cAMP dependent protein kinase catalytic subunit. Tartu, 2017, 115 p.
168. **Agnes Heering**. Experimental realization and applications of the unified acidity scale. Tartu, 2017, 123 p.
169. **Delia Juronen**. Biosensing system for the rapid multiplex detection of mastitis-causing pathogens in milk. Tartu, 2018, 85 p.
170. **Hedi Rahnel.** ARC-inhibitors: from reliable biochemical assays to regulators of physiology of cells. Tartu, 2018, 176 p.
171. **Anton Ruzanov.** Computational investigation of the electrical double layer at metal–aqueous solution and metal–ionic liquid interfaces. Tartu, 2018, 129 p.
172. **Katrin Kestav.** Crystal Structure-Guided Development of Bisubstrate-Analogue Inhibitors of Mitotic Protein Kinase Haspin. Tartu, 2018, 166 p.
173. **Mihkel Ilisson.** Synthesis of novel heterocyclic hydrazine derivatives and their conjugates. Tartu, 2018, 101 p.
174. **Anni Allikalt.** Development of assay systems for studying ligand binding to dopamine receptors. Tartu, 2018, 160 p.
175. **Ove Oll.** Electrical double layer structure and energy storage characteristics of ionic liquid based capacitors. Tartu, 2018, 187 p.
176. **Rasmus Palm.** Carbon materials for energy storage applications. Tartu, 2018, 114 p.
177. **Jörgen Metsik.** Preparation and stability of poly(3,4-ethylenedioxythiophene) thin films for transparent electrode applications. Tartu, 2018, 111 p.
178. **Sofja Tšepelevitš.** Experimental studies and modeling of solute-solvent interactions. Tartu, 2018, 109 p.
179. **Märt Lõkov.** Basicity of some nitrogen, phosphorus and carbon bases in acetonitrile. Tartu, 2018, 104 p.
180. **Anton Mastitski**. Preparation of α-aza-amino acid precursors and related compounds by novel methods of reductive one-pot alkylation and direct alkylation. Tartu, 2018, 155 p.
181. **Jürgen Vahter**. Development of bisubstrate inhibitors for protein kinase CK2. Tartu, 2019, 186 p.

182. **Piia Liigand.** Expanding and improving methodology and applications of ionization efficiency measurements. Tartu, 2019, 189 p.
183. **Sigrid Selberg.** Synthesis and properties of lipophilic phosphazene-based indicator molecules. Tartu, 2019, 74 p.
184. **Jaanus Liigand.** Standard substance free quantification for LC/ESI/MS analysis based on the predicted ionization efficiencies. Tartu, 2019, 254 p.
185. **Marek Mooste.** Surface and electrochemical characterisation of aryl film and nanocomposite material modified carbon and metal-based electrodes. Tartu, 2019, 304 p.
186. **Mare Oja.** Experimental investigation and modelling of pH profiles for effective membrane permeability of drug substances. Tartu, 2019, 306 p.
187. **Sajid Hussain.** Electrochemical reduction of oxygen on supported Pt catalysts. Tartu, 2019, 220 p.
188. **Ronald Väli.** Glucose-derived hard carbon electrode materials for sodium-ion batteries. Tartu, 2019, 180 p.
189. **Ester Tee.** Analysis and development of selective synthesis methods of hierarchical micro- and mesoporous carbons. Tartu, 2019, 210 p.
190. **Martin Maide.** Influence of the microstructure and chemical composition of the fuel electrode on the electrochemical performance of reversible solid oxide fuel cell. Tartu, 2020, 144 p.
191. **Edith Viirlaid.** Biosensing Pesticides in Water Samples. Tartu, 2020, 102 p.
192. **Maike Käärik.** Nanoporous carbon: the controlled nanostructure, and structure-property relationships. Tartu, 2020, 162 p.
193. **Artur Gornischeff.** Study of ionization efficiencies for derivatized compounds in LC/ESI/MS and their application for targeted analysis. Tartu, 2020, 124 p.
194. **Reet Link.** Ligand binding, allosteric modulation and constitutive activity of melanocortin-4 receptors. Tartu, 2020, 108 p.
195. **Pilleriin Peets.** Development of instrumental methods for the analysis of textile fibres and dyes. Tartu, 2020, 150 p.